Open Access Indonesian Journal of Medical Reviews
Volume 6, Issue 6, 2026 | Article ID: 1000 | Pages: 649–665 | e-ISSN 2807-6257
OAIJMR

CASE REPORT

Longitudinal Volumetric Trajectory, Trans-Midline Sinonasal Osteolysis, and Stage IV Progression Following Inadvertent Evisceration and Delayed Adjuvant Chemotherapy in Recurrent Orbital Malignant Melanoma: An Observational Analytic Case Study

I Gusti Ngurah Agung Wisnu Kresnan Dana[1], Putu Yuliawati[1*], Ni Made Laksmi Utari[1], I Wayan Losen Adnyana[2]

[1] Reconstructive Oculoplastic and Oncology Division, Department of Ophthalmology, Faculty of Medicine, Universitas Udayana / Prof. Dr. I.G.N.G. Ngoerah General Hospital, Denpasar, Indonesia

[2] Medical Hemato-Oncology Division, Department of Internal Medicine, Faculty of Medicine, Universitas Udayana / Prof. Dr. I.G.N.G. Ngoerah General Hospital, Denpasar, Indonesia

ARTICLE INFO

Article history

Received: September 20, 2026
Revised: October 15, 2026
Accepted: October 30, 2026
Available Online: November 12, 2026
Published: December 1, 2026

Keywords

dacarbazine; inadvertent evisceration; orbital exenteration; orbital melanoma; case report

***Corresponding author**

Putu Yuliawati
E-mail: putu.yulia@unud.ac.id

DOI

https://doi.org/10.37275/oaijmr.v6i6.1000

Access license

CC BY-NC-SA 4.0: readers may share and adapt the work for non-commercial purposes with attribution, indication of changes, and the same license.

Copyright

© 2026 The Authors. Published by HM Publisher in collaboration with CMHC Research Center.

ABSTRACT

Background: Orbital malignant melanoma is an aggressive craniofacial malignancy. Scleral disruption at evisceration and delayed systemic therapy may precede local relapse and metastasis.

Objective: To describe the volumetric course and staging evolution of a neglected recurrent orbital melanoma.

Methods: A 56-year-old female farmer was followed for 31.5 months (August 2023 to March 2026) at Prof. Dr. I.G.N.G. Ngoerah General Hospital, Indonesia, across eight epochs (T_0 to T_7). Tumor volume was calculated by ellipsoid volumetry ($V = [\pi/6] \times L \times W \times H$) and described by percentage change (Δ%), specific growth rate (SGR), and doubling time (Td). No inferential statistics were applied.

Result: After inadvertent right ocular evisceration for presumed bulbar prolapse (T_0) and semi-enucleation confirming melanoma (T_1), a 6-month referral delay was followed by a 4.80 × 4.60 × 4.20 cm (48.56 cm^3) Stage IIIC (cT4eN0M0) orbital mass invading the optic nerve and extraocular muscles (T_2). Radical orbital exenteration (T_3) showed epithelioid melanoma with tumor-positive (R1/R2) bony margins. The patient repeatedly refused adjuvant dacarbazine. A 2.95 cm^3 socket relapse appeared at T_5. Over 210 untreated days the volume rose 44.42-fold (Δ% = +4,341.69%; SGR = 1.81%/day; Td = 38.37 days) to a 6.50 × 7.00 × 5.50 cm (131.03 cm^3) mass with bilateral sinonasal destruction, inferoauricular lymphadenopathy, and suspected pulmonary metastasis (Stage IV, cT4eN1M1; T_6).

Conclusion: In this patient, inadvertent evisceration and non-adherence to chemotherapy for socioeconomic reasons were followed by rapid osteolytic recurrence and Stage IV dissemination. One case cannot show causation.

1. Introduction

Ocular and adnexal malignant melanomas form a biologically varied group of neural crest-derived tumors. They arise from melanocytes of the uveal tract, conjunctival epithelium, eyelid dermis, lacrimal drainage system and orbital soft tissue.[1,2] Registry data from the American College of Surgeons Commission on Cancer and from international ocular oncology groups give the distribution: primary cutaneous melanoma accounts for about 91.0% of all diagnosed melanomas, ocular melanoma for 5.0%, mucosal melanoma for 1.0% and melanoma of unknown primary origin for 2.0%.[3,4] Posterior uveal melanoma is the most common primary intraocular cancer in adults, with about 85.0% arising in the choroid and 10.0% to 12.0% in the ciliary body, whereas iris melanoma makes up only 3.0% to 5.0% of uveal cases, and the annual age-standardized incidence is about 5.0 per million population in Western cohorts and 0.2 to 0.6 per million across Asian populations.[5,6] More than 97.0% of patients with primary uveal melanoma have localized intraocular disease at diagnosis. Even so, the tumor spreads readily through the blood. The liver is the usual target. Long-term metastatic mortality depends largely on the initial tumor dimensions, the cytogenetic profile and the timeliness of primary local control.[7]

Melanoma confined to the orbit is much rarer than intraocular uveal melanoma. It is also harder to manage. Two forms are recognized: primary orbital melanoma (POM) and secondary orbital melanoma (SOM). Primary orbital melanoma arises de novo from ectopic neural crest melanocytes along the ciliary nerves, the scleral emissary vessels or the leptomeningeal sheaths of the optic nerve. It accounts for less than 1.0% of all orbital neoplasms. Only a limited number of histopathologically verified cases have been documented worldwide, and many are associated with congenital ocular melanocytosis (Nevus of Ota) or cellular blue nevi.[8,9] Secondary orbital melanoma is considerably more frequent and represents 5.0% to 10.0% of all secondary orbital malignancies. It develops by direct extrascleral extension of a choroidal or ciliary body melanoma. It can also follow deep stromal invasion from a neglected conjunctival or eyelid melanoma, contiguous spread from a paranasal sinus mucosal melanoma, or hematogenous metastasis from a

distant cutaneous site. In a retrospective cohort of 37 patients with orbital melanoma at Beijing Tongren Hospital, secondary invasion came most often from primary conjunctival melanoma (32.4%), followed by extrascleral extension of uveal melanoma (29.7%), eyelid melanoma (21.6%), primary orbital melanoma (10.8%) and lacrimal sac melanoma (5.4%).[2]

In resource-limited settings, two vulnerabilities govern the course and operability of orbital malignant melanoma. The first is iatrogenic violation of the ocular coats at the first misdiagnosis. The second is patient-driven postponement of definitive multimodal oncologic care.[10] Evisceration is strictly contraindicated in an eye that may harbor an intraocular malignancy. Transecting the cornea and curetting the contents breaches the scleral barrier. Viable tumor nests remain in the intrascleral emissary channels, and malignant melanocytes can spread mechanically through the extrascleral orbital fat and periosteum. The error is termed inadvertent evisceration. It typically occurs when a blind, painful eye with opaque media, secondary neovascular glaucoma or tumor necrosis and inflammation resembles acute panophthalmitis, endophthalmitis or spontaneous bulbar perforation. The eye is then operated on without preoperative B-mode ultrasonography or contrast-enhanced orbital magnetic resonance imaging (MRI).[11] Later, the patient may decline metastatic staging, radical clearance of surgical margins, postoperative orbital radiotherapy and systemic adjuvant therapy, often because of rural isolation and socioeconomic hardship, and microscopic residual disease then proliferates rapidly across the craniofacial skeleton.[8]

Advanced orbital melanoma is lethal, yet the literature on it consists mostly of descriptive case reports and pooled survival series that do not model the regrowth of untreated tumor in vivo with serial volume measurements.[12,13] To our knowledge, no earlier report from Southeast Asia has quantified three parameters in one patient: the serial ellipsoid volume, the exponential specific growth rate (SGR) and the tumor volume doubling time (Td). The disease course in question ran from inadvertent evisceration, through tumor-positive (R1/R2) radical orbital exenteration, to trans-midline sinonasal osteolysis. It ended in American Joint Committee on Cancer (AJCC) 8th edition Stage IV (cT4eN1M1) disease during prolonged refusal of chemotherapy.[14] This case report brings together several elements: serial three-dimensional volumetric kinetics, multiparametric craniofacial CT and MRI mapping of osteolysis, histopathologic correlation of epithelioid cherry-red macronucleolar architecture, and Naranjo pharmacovigilance scoring. The study aimed to evaluate the clinicopathologic consequences, volumetric growth kinetics, sinonasal and skull-base invasion patterns and staging evolution of two-stage diagnostic and therapeutic delay. The patient had neglected recurrent orbital malignant melanoma and was managed at a tertiary academic referral center in Indonesia.

2. Methods

2.1. Study design and setting

This was a single-patient case report with a retrospective phase and a prospective phase. Two phases were combined. The first was a retrospective reconstruction of the clinical timeline (August 2023 to December 2024). The second was prospective clinicopathologic, radiologic, surgical and oncologic follow-up from January 2025 through March 2026. The study took place in the Reconstructive Oculoplastic and Oncology (ROO) Division, Department of Ophthalmology. Collaborating units were the Medical Hemato-Oncology (HOM) Division of the Department of Internal Medicine and the Departments of Radiology and Anatomical Pathology at Prof. Dr. I.G.N.G. Ngoerah General Hospital (formerly Sanglah General Hospital), Faculty of Medicine, Udayana University, Denpasar, Bali, Indonesia. The report follows the CARE reporting guideline[15], and eight sequential clinical observation epochs (T_0 to T_7) covered a total observation window of 31.5 months (945 days).

2.2. Participants and eligibility

The study enrolled one adult female agricultural worker. She was referred to the tertiary ocular oncology service with histopathologically confirmed recurrent malignant melanoma of the right orbit (oculus dexter, OD). At a secondary regional hospital she had earlier undergone non-oncologic ocular evisceration (T_0, August 2023). She had then undergone excision of a secondary orbital mass with removal of the residual scleral shell (T_1, 25 June 2024). Diagnosis of recurrent orbital malignant melanoma at the tertiary center required concordant clinical, radiologic and histopathologic evidence, beginning with a progressive, firm, lobulated intraorbital and periorbital soft-tissue mass in an anophthalmic socket and continuing with contrast-enhanced orbital computed tomography (CT) and multiparametric contrast-enhanced magnetic resonance imaging (MRI) that showed invasive replacement of orbital and sinonasal soft tissue with cortical bone destruction. Histopathology completed the criteria. Hematoxylin and Eosin (H&E, 400× magnification) staining of the en bloc orbital exenteration specimen had to show sheets of malignant epithelioid melanocytes with cytoplasmic melanin pigment, prominent cherry-red macronucleoli, a high nuclear-to-cytoplasmic (N/C) ratio and frequent mitotic figures.[16]

2.3. Variables and data collection

Serial clinical, ophthalmic, radiologic and biochemical evaluations were recorded across eight defined observation epochs. T_0 (Month 0.0, August 2023) was the initial presentation. The patient had a painful blind right eye and underwent inadvertent evisceration at the secondary hospital. T_1 (Month 10.0, 25 June 2024) was the first socket recurrence. Semi-enucleation confirmed malignant melanoma, and the patient initially refused metastatic staging. T_2 (Months 16.5–17.0, 26 December 2024 to 21 January 2025) was the tertiary referral presentation, with contrast-enhanced axial and coronal orbital CT and a baseline posteroanterior chest radiograph. T_3 (Month 17.5, 30 January to 10 February 2025) comprised radical right orbital exenteration under general anesthesia with orotracheal intubation. It also included clinical evaluation on Postoperative Day 8 (7 February 2025), histopathologic margin reporting on 10 February 2025 and refusal of adjuvant dacarbazine chemotherapy. T_4 (Month 18.5, 11 March 2025) was the 6-week post-exenteration socket evaluation. Systemic therapy was again refused. T_5 (Month 24.0, 4 August to 14 August 2025) was the frank medial orbital relapse 6 months after exenteration, with multiparametric axial, coronal and sagittal contrast head and orbital MRI on 14 August 2025, after which chemotherapy was deferred for 7 months. T_6 (Month 31.0, 2 March to 12 March 2026) was the massive craniofacial progression 13.5 months after exenteration. It included assessment of regional inferoauricular lymphadenopathy, repeat multiparametric contrast head and orbital MRI, a repeat posteroanterior chest radiograph on 2 March 2026 and hepatorenal biochemical profiling. T_7 (Month 31.5, late March 2026) was the completion of Cycle 1 of intravenous dacarbazine chemotherapy and the transition to community palliative care

at Tabanan Regional Hospital. At each tertiary visit the contralateral left eye (oculus sinister, OS) was examined. Tests were Snellen best-corrected visual acuity (BCVA) with pinhole testing (PHNI), Goldmann or non-contact applanation tonometry for intraocular pressure (IOP, mmHg), slit-lamp biomicroscopy and dilated indirect ophthalmoscopy.

Anatomic disease extent at each epoch was classified with the American Joint Committee on Cancer (AJCC) 8th Edition Tumor-Node-Metastasis (TNM) system for uveal melanoma, applied by analogy because the tumor origin could not be determined. The National Comprehensive Cancer Network (NCCN, Version 2.2026) and United Kingdom national uveal melanoma guidelines were used alongside it. The inadvertent evisceration at T_0 destroyed the primary globe architecture, so the basal diameter and apical thickness of the tumor in the choroid or ciliary body could not be measured retrospectively. This shaped the staging. T-category assignment at T_2, T_5 and T_6 was based instead on the size of the extrascleral and orbital soft-tissue and bony extension (category T4e, defined as extrascleral extension > 5.0 mm). Tumor dimensions were compared with the plaque-brachytherapy feasibility limits for eye-sparing treatment, referred to here as the COMS limits (Collaborative Ocular Melanoma Study). These are a maximum basal diameter of ≤ 19.0 mm and an apical thickness of ≤ 10.0 mm for a 23.0 mm radioisotope plaque, and the dimensions were also compared with published cohorts of primary and secondary orbital melanoma treated by radical orbital exenteration.[17]

2.4. Statistical analysis

Only one patient was studied (n = 1), so no inferential hypothesis tests were applied. This excluded p-values, Student t-tests, analysis of variance and chi-square tests. Disease dynamics were described with exact three-dimensional ellipsoid volumetry, serial percentage change (Δ%), the exponential specific growth rate (SGR), the tumor volume doubling time (Td) and ratios to the COMS plaque limits (× limit), while Reference Change Value (RCV) monitoring tracked the stability of the contralateral eye and formal algorithmic causality and pharmacovigilance instruments were also used. Tumor volume (V, in cm^3) was computed from orthogonal clinical caliper or multiplanar CT/MRI dimensions (length L, width W and height or depth H, in cm). V_2 was calculated from the external caliper measurement of 21 January 2025 and from the CT dimensions of 26 December 2024, and V_5 and V_6 from the dimensions recorded at the clinical visits of 4 August 2025 and 2 March 2026. The prolate ellipsoid equation was $V = (\pi / 6) \times L \times W \times H \approx 0.523599 \times L \times W \times H$. The relative change from a reference volume (V_ref, the T_2 volume or the T_5 nadir) to a later volume (V_n) was $\Delta\% = [(V_n - V_{ref}) / V_{ref}] \times 100\%$. For the 210-day untreated recurrence interval from T_5 (4 August 2025, V_5) to T_6 (2 March 2026, V_6), the specific growth rate was $SGR = [\ln(V_6 / V_5) / (t_6 - t_5)] \times 100\%$ (in %/day). The doubling time was $Td = [\ln(2) \times (t_6 - t_5)] / \ln(V_6 / V_5)$ (in days). The sequence of surgical and treatment events and of tumor progression is described narratively. Tolerability of Cycle 1 dacarbazine at T_7 was assessed with the Naranjo Adverse Drug Reaction (ADR) Probability Scale and the World Health Organization–Uppsala Monitoring Centre (WHO-UMC) causality categories.

2.5. Ethical approval

The study protocol received ethical clearance from the CMHC Research Center Ethics Committee, Indonesia (Protocol Approval Number: 2026/0418). It was conducted in accordance with the World Medical Association Declaration of Helsinki (2013 revision) and the International Committee of Medical Journal Editors (ICMJE) Recommendations for the Protection of Research Participants. The patient and her legal family representative gave written informed consent for radical surgery, histopathologic examination, serial diagnostic imaging, systemic chemotherapy and the publication of anonymized clinical data and diagnostic photographs. Privacy requirements of the ICMJE and the Committee on Publication Ethics (COPE) were met in two ways. All clinical facial and periocular photographs were de-identified with solid black bars over the contralateral ocular and periocular identifying landmarks, leaving the index orbital lesion visible. All Picture Archiving and Communication System (PACS) patient headers were masked before the manuscript was compiled.

3. Results

3.1. Pre-referral course, inadvertent evisceration (T_0), and refusal of staging (T_1)

The patient was a 56-year-old Indonesian female farmer from rural Tabanan Regency, Bali. On 21 January 2025 (Epoch T_2) she was referred to the Reconstructive Oculoplastic and Oncology (ROO) clinic at Prof. Dr. I.G.N.G. Ngoerah General Hospital. She had a progressively enlarging, painful right orbital mass in an anophthalmic socket. Her occupational history recorded unprotected daily solar ultraviolet (UV-A and UV-B) exposure of more than 6.0 to 8 hours per day. This had lasted more than three decades of open-field farming. She denied any personal or family history of cutaneous melanoma, dysplastic nevus syndrome, congenital ocular melanocytosis (Nevus of Ota), systemic hypertension, diabetes mellitus or drug allergy. In 2021 her left eye had undergone combined trabeculectomy with peripheral iridectomy at the 11 o'clock meridian. Phacoemulsification with posterior chamber intraocular lens (PCIOL) implantation was done in the same eye for primary glaucoma and cataract.

Her earlier surgical history showed a two-stage diagnostic and therapeutic delay of 17 months before tertiary presentation. In August 2023 (Epoch T_0, Month 0.0) she presented to a secondary regional hospital with severe acute right ocular pain (Numerical Rating Scale, NRS 8/10). Intraocular pressure was clearly raised. A dark brown-to-black tissue mass protruded anteriorly through the globe. No B-scan ocular ultrasonography or contrast-enhanced orbital MRI was done to exclude an intraocular neoplasm. The condition was diagnosed clinically as non-neoplastic right bulbar prolapse. She underwent immediate ocular evisceration with wide local tissue excision. No histopathologic record of the eviscerated intraocular contents was obtained. This destroyed the intact scleral-uveal landmarks needed to tell a primary choroidal or ciliary body melanoma from a secondary adnexal melanoma. Ten months later, in June 2024 (Epoch T_1, Month 10.0), she returned to the secondary facility. Her right socket was swelling progressively and had pushed out her ocular prosthesis. On 25 June 2024 she underwent secondary excision of the orbital mass with removal of the residual scleral shell (semi-enucleation). Histopathologic analysis of the tissue established the diagnosis of malignant melanoma. She was urgently advised to undergo tertiary systemic metastatic staging and multidisciplinary oncology management. She refused referral. She was lost to medical follow-up for 6.0 consecutive months (June 2024 to December 2024), as detailed in Table 1.

Table 1. Clinicopathologic, ophthalmic, and surgical course across observation epochs (T_0 to T_7, August 2023 to March 2026) in recurrent orbital malignant melanoma.

Observation Epoch & Date	Elapsed Time (Months)	Right Orbit (OD) Clinical & Pathological Status	Left Eye (OS) Functional & Anatomical Status	AJCC 8th Edition TNM & Stage	Surgical / Oncological Intervention & Adherence Outcome
T_0: Initial Presentation (August 2023, Secondary Hospital)	0.0 mo (Baseline)	Severe right ocular pain (NRS 8/10), elevated IOP, dark protruding intraocular uveal mass clinically misdiagnosed as bulbar prolapse; no pre-operative B-scan US or MRI performed	BCVA 6/9.5 PHNI; history of trabeculectomy + phacoemulsification + PCIOL (2021); quiet anterior segment; normal fundus	Unstaged (pTX NX MX; origin obscured)	Inadvertent ocular evisceration + wide mass excision without histopathological origin confirmation; iatrogenic scleral disruption
T_1: First Orbital Relapse (25 June 2024, Secondary Hospital)	10.0 mo	Progressive right anophthalmic socket swelling; inability to retain ocular prosthesis; firm recurrent intraorbital mass	BCVA 6/9.5 PHNI; flat filtering bleb; clear cornea; deep AC; PI (+) at 11 o'clock; PCIOL stable	Recurrent local orbital tumor (cT4e NX MX)	Orbital mass excision & residual scleral removal (semi-enucleation); histopathology confirmed malignant melanoma; patient refused metastatic workup (6-mo delay)
T_2: Tertiary Referral (26 Dec 2024 – 21 Jan 2025, Prof. Ngoerah General Hospital)	16.5–17.0 mo	Anophthalmic socket, NLP; palpebral proptosis with telangiectasia & chemosis; firm lobulated mass 4.50 × 4.00 × 2.50 cm (V = 23.56 cm^3); CT mass 4.80 × 4.60 × 4.20 cm (V = 48.56 cm^3) invading ON & EOM	BCVA 6/9.5 PHNI; normal lids; quiet conjunctiva; clear cornea; deep AC; PI (+); PCIOL in situ; full extraocular motility without pain; IOP 11 mmHg	cT4e cN0 cM0 (Stage IIIC; indeterminate RLL solitary lung nodule)	Multidisciplinary staging (contrast orbital CT, chest PA radiograph); planned radical right orbital exenteration & HOM adjuvant chemotherapy
T_3: Exenteration & PA (30 Jan – 10 Feb 2025, Prof. Ngoerah General Hospital)	17.5 mo	Intraoperative medial & inferior orbital wall bony destruction excised; POD 8 (7 Feb 2025): minimal pain (NRS 2/10), intact Prolene 4-0 sutures, residual bony infiltration; PA (10 Feb 2025): epithelioid melanoma, cherry-red nucleoli, R1/R2 positive margins	BCVA 6/7.5; quiet anterior segment; PCIOL (+); IOP 12 mmHg; cup-to-disc ratio and retinal vasculature normal	pT4e cN0 cM0 (Stage IIIC)	Total right orbital exenteration under GA-OTT + bony wall debridement + gentamicin tamponade; patient refused HOM adjuvant dacarbazine and IHC
T_4: Early Post-Op Check (11 March 2025, Prof. Ngoerah General Hospital)	18.5 mo (1.5 mo post-exenteration)	Anophthalmic exenterated socket with mild purulent exudate on gauze packing and persistent medial/inferior bony wall tumor infiltration	BCVA 6/9.5 PHNI; flat conjunctival bleb; clear cornea; PI (+) at 11 o'clock; deep AC; PCIOL (+); IOP 10 mmHg	pT4e cN0 cM0 (Stage IIIC; persistent R1/R2 bed)	Local wound care with gentamicin dressing; patient persistently refused systemic chemotherapy & requested transfer to secondary hospital
T_5: Frank Socket Relapse (4 Aug – 14 Aug 2025, Prof. Ngoerah General Hospital)	24.0 mo (6.0–6.5 mo post-exenteration)	Firm, non-tender recurrent medial orbital mass 2.50 × 1.50 × 1.50 cm (V = 2.95 cm^3) with surface crusting; MRI (14 Aug 2025): multifocal heterogeneous recurrence invading right ethmoid/frontal sinuses, sphenoid greater wing, frontal/nasal bones & lamina papyracea	BCVA 6/9.5 PHNI; stable anterior segment; flat bleb; PI (+); PCIOL (+); IOP 11 mmHg; Fazekas Grade I cerebral white matter changes on MRI	rT4e cN0 cM0 (Recurrent Stage IIIC)	Contrast head/orbital MRI confirmed osteolytic sinonasal recurrence; HOM re-planned Dacarbazine, but patient delayed therapy for 7 months
T_6: Massive Progression (2 Mar – 12 Mar 2026, Prof. Ngoerah General Hospital)	31.0 mo (13.5 mo post-exenteration)	Massive exophytic ulcerated/hyperemic right orbital mass 6.50 × 7.00 × 5.50 cm (V = 131.03 cm^3) with ipsilateral CN V1/V2 facial paresthesia; two mobile right inferoauricular lymph nodes (1.00 × 2.00 × 1.00 cm & 1.00 × 1.00 × 1.00 cm); bilateral lamina papyracea & sinus destruction on MRI	BCVA 6/9.5 PHNI; quiet conjunctiva; flat bleb; clear cornea; deep AC; round pupil with PI (+) at 11 o'clock; PCIOL stable; IOP 11 mmHg	cT4e cN1 cM1 (Stage IV; nodal + right lung metastasis)	Chest radiograph raised suspicion of right pulmonary metastasis; AST/ALT & renal function normal; HOM initiated systemic Dacarbazine protocol
T_7: Palliative Transition (Late March 2026, Tabanan Regional Hospital)	31.5 mo (14.0 mo post-exenteration)	Persistently advanced craniofacial tumor burden post-Cycle 1 chemotherapy; intermittent mild orbital pain controlled with oral analgesics; ambulatory status (ECOG 1)	BCVA 6/9.5 PHNI; preserved functional vision enabling independent daily agricultural activities	cT4e cN1 cM1 (Stage IV; palliative care)	Completed 1 cycle of IV Dacarbazine (DTIC); elected discontinuation of Cycle 2–3 due to travel/accommodation costs; transferred to rural palliative care

Abbreviations: AC, anterior chamber; AJCC, American Joint Committee on Cancer; ALT, alanine aminotransferase; AST, aspartate aminotransferase; BCVA, best-corrected visual acuity; CT, computed tomography; DTIC, dacarbazine; ECOG, Eastern Cooperative Oncology Group; EOM, extraocular muscles; GA-OTT, general anesthesia with orotracheal tube; HOM, Medical Hemato-Oncology Division; IHC, immunohistochemistry; IOP, intraocular pressure; MRI, magnetic resonance imaging; NLP, no light perception; NRS, Numerical Rating Scale; OD, oculus dexter (right eye); ON, optic nerve; OS, oculus sinister (left eye); PA, posteroanterior; PCIOL, posterior chamber intraocular lens; PHNI, pinhole no improvement; PI, peripheral iridectomy; POD, postoperative day; RLL, right lower lobe; US, ultrasonography; V, ellipsoid tumor volume. Elapsed times are approximate.

3.2. Tertiary referral and CT staging (T_2)

At tertiary evaluation on 21 January 2025 (Epoch T_2, Month 17.0), the patient reported severe right orbital pain (NRS 7/10). It radiated to the ipsilateral frontal and temporal regions of the head and had worsened over the preceding 3 months. Marked lid swelling was present, without purulent discharge or epiphora. Examination of the right orbit (OD) showed an anophthalmic socket with No Light Perception (NLP). There was prominent palpebral proptosis with overlying cutaneous telangiectasia and severe conjunctival chemosis. A firm, lobulated (bosselated) solid mass filled the orbital cavity. Its anterior surface was smooth and palpation tenderness was minimal. External caliper measurement gave 4.50 × 4.00 × 2.50 cm, an ellipsoid clinical mass volume of V = 23.56 cm^3. The contralateral left eye (OS) had a best-corrected visual acuity (BCVA) of 6/9.5 PHNI. The eyelids were normal and the conjunctiva was quiet, with a flat superior filtering bleb. The cornea was clear and the anterior chamber deep. The pupil was regular and round with a patent peripheral iridectomy at 11 o'clock, and the PCIOL was stable in situ. The posterior pole was normal on fundoscopy, extraocular motility was full and pain-free in all cardinal gazes, and intraocular pressure was a normal 11 mmHg. The head and neck examination found no palpable cervical, preauricular or submandibular lymphadenopathy (cN0). Contrast-enhanced orbital CT on 26 December 2024 showed a large, lobulated, heterogeneous solid mass. It completely replaced the right orbital cavity and measured 4.80 × 4.60 × 4.20 cm (ellipsoid radiologic tumor volume V = 48.56 cm^3, which is +106.11% larger than the clinical volume; the CT preceded the caliper measurement by 26 days, so the two volumes were not obtained on the same date). The mass could not be separated from the right optic nerve and all right extraocular muscles and infiltrated them directly. There was early cortical erosion of the medial and inferior orbital walls, and the tumor extended toward the right ethmoid-frontal sinus complex. No intracranial parenchymal invasion, cerebral infarction or hemorrhage was seen. Baseline posteroanterior chest radiography on 21 January 2025 showed aortic atherosclerosis, thoracic spondylosis and an indeterminate solitary pulmonary nodule in the right lower lung zone. There were no osteolytic rib or vertebral metastases (cM0). The

baseline tertiary stage was therefore AJCC 8th edition Stage IIIC (cT4eN0M0), as illustrated in Figure 1.

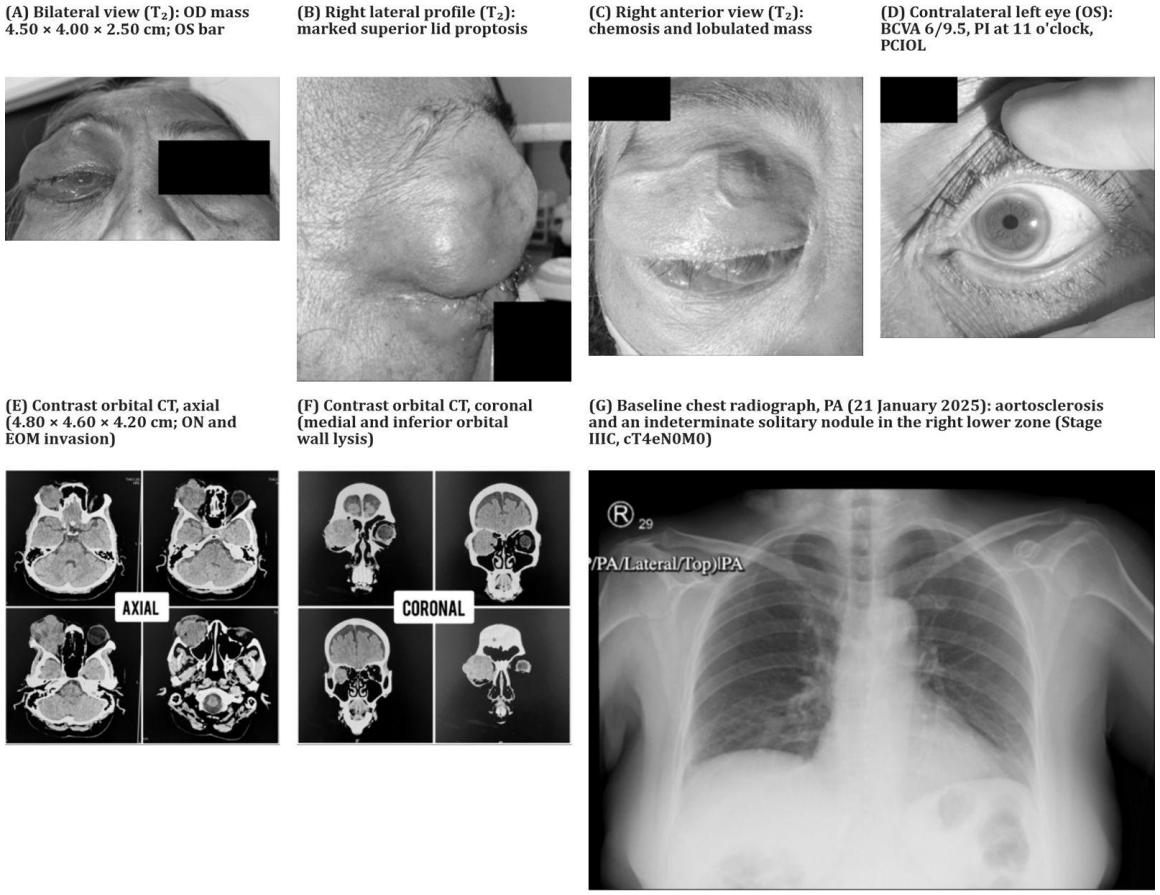


Figure 1. Baseline tertiary referral presentation (T_2, December 2024 to January 2025): (A–C) right orbital anophthalmic socket with palpebral proptosis, telangiectasia, chemosis, and a firm lobulated 4.50 × 4.00 × 2.50 cm (V = 23.56 cm^3) recurrent melanoma mass; (D) contralateral pseudophakic left eye (OS: BCVA 6/9.5 PHNI, 11 o'clock peripheral iridectomy, IOP 11 mmHg); (E, F) axial and coronal contrast-enhanced orbital CT (26 December 2024) showing a 4.80 × 4.60 × 4.20 cm (V = 48.56 cm^3) solid mass replacing the right globe, with optic nerve, extraocular muscle, and medial and inferior bony wall invasion; (G) baseline posteroanterior chest radiograph (21 January 2025) showing aortosclerosis and a right lower zone solitary nodule (Stage IIIC, cT4eN0M0). Facial features are masked with black bars (ICMJE/COPE).

Compared with the COMS limits for plaque brachytherapy (largest basal diameter ≤ 19.0 mm and apical thickness ≤ 10.0 mm for the largest 23.0 mm radioisotope plaque), the pre-exenteration tumor dimensions at T_2 far exceeded every physical threshold for conservative eye-sparing or socket-sparing radiotherapy. The clinical mass had a basal diameter of 45.0 mm (2.37 × limit) and a thickness of 25.0 mm (2.50 × limit). The CT mass was larger still. Its basal diameter was 48.0 mm (2.53 × limit) and its vertical thickness 42.0 mm (4.20 × limit). It also invaded the optic nerve, the extraocular muscles and the bony walls directly, as detailed in Table 2.

Table 2. Tumor dimensions, ellipsoid volume (V = [π/6] × L × W × H), percentage change (Δ%), specific growth rate (SGR), and doubling time (Td).

Morphometric Parameter & Measurement Modality	T_2 Referral Clinical (21 Jan 2025)	T_2 Pre-Op CT Scan (26 Dec 2024)	T_5 Socket Recurrence (4 Aug 2025)	T_6 Massive Relapse (2 Mar 2026)	Interval Kinetic Trajectory & Biostatistical Comparison
Linear Dimensions: L × W × H (cm)	4.50 × 4.00 × 2.50 cm (External caliper)	4.80 × 4.60 × 4.20 cm (Contrast orbital CT)	2.50 × 1.50 × 1.50 cm (Medial socket nodule)	6.50 × 7.00 × 5.50 cm (Exophytic craniofacial)	Maximum linear diameter increased +180.00% during T_5→T_6 (2.50 → 7.00 cm)
Maximum Basal Diameter vs COMS Plaque Limit (≤ 19.0 mm)	45.0 mm (2.37 × plaque limit)	48.0 mm (2.53 × plaque limit)	25.0 mm (1.32 × plaque limit)	70.0 mm (3.68 × plaque limit)	Exceeded largest 23.0 mm plaque capacity (19.0 mm tumor limit) at all epochs
Apical / Vertical Thickness vs COMS Plaque Limit (≤ 10.0 mm)	25.0 mm (2.50 × thickness limit)	42.0 mm (4.20 × thickness limit)	15.0 mm (1.50 × thickness limit)	55.0 mm (5.50 × thickness limit)	Precluded globe-sparing brachytherapy or proton beam therapy across all stages
Ellipsoid Tumor Volume: V = (π/6) × L × W × H (cm^3)	23.56 cm^3 (Baseline clinical V_2clin)	48.56 cm^3 (Baseline CT V_2CT)	2.95 cm^3 (Early relapse V_5)	131.03 cm^3 (Advanced relapse V_6)	Net expansion: +456.15% vs T_2 clinical (5.56×); +169.83% vs T_2 CT (2.70×)

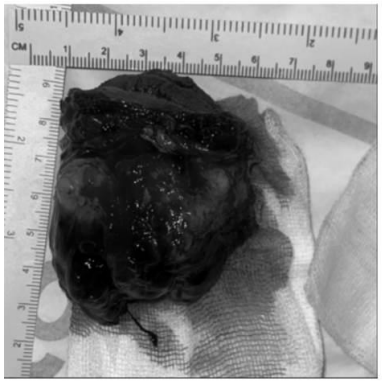
Morphometric Parameter & Measurement Modality	T_2 Referral Clinical (21 Jan 2025)	T_2 Pre-Op CT Scan (26 Dec 2024)	T_5 Socket Recurrence (4 Aug 2025)	T_6 Massive Relapse (2 Mar 2026)	Interval Kinetic Trajectory & Biostatistical Comparison
Untreated Relapse Volumetric Surge: Δ% ($T_5 \rightarrow T_6$, 210 Days)	Reference pre-op clinical baseline	Debulked via radical exenteration at T_3	Baseline post-exenteration recurrence (100.0%)	+4,341.69% volumetric expansion (44.42-fold)	Absolute volumetric gain ΔV = +128.08 cm^3 over 210 days (+0.61 cm^3/day)
Exponential Specific Growth Rate: SGR = $\ln(V_6/V_5)/\Delta t$ (%/day)	Not calculable (T_1 volume not reported)	Resected at T_3 (R1/R2 bony margin)	Onset of untreated exponential phase	1.81%/day ($k = 0.0181\ day^{-1}$)	Rapid growth in a tumor with epithelioid cytology and prominent nucleoli
Tumor Volume Doubling Time: Td = $[\ln(2) \times \Delta t]/\ln(V_6/V_5)$ (Days)	Not calculable (T_1 volume not reported)	Surgical cytoreduction to microscopic R1 bed	Post-exenteration regrowth lag (186 days)	38.37 days (5.47 volume doublings)	Accelerated doubling time (38.37 days) during 7-month chemotherapy refusal
Regional Lymph Node Burden: Right Inferoauricular (cm / cm^3)	Non-palpable (0.00 cm^3; cN0)	No cervical/parotid adenopathy (cN0)	Non-palpable (0.00 cm^3; cN0)	Node 1: 1.00 × 2.00 × 1.00 cm (1.05 cm^3) Node 2: 1.00 × 1.00 × 1.00 cm (0.52 cm^3)	Total nodal volume 1.57 cm^3 at T_6; triggered transition from cN0 to cN1 (Stage IV)

Formulas: Ellipsoid volume $V = (\pi/6) \times L \times W \times H \approx 0.523599 \times L \times W \times H$. Serial percentage change $\Delta\% = [(Vn - V0) / V0] \times 100\%$. Specific growth rate $SGR = [\ln(V6 / V5) / (t6 - t5)] \times 100\%$, where V5 = 2.95 cm^3, V6 = 131.03 cm^3, and Δt = 210 days (4 August 2025 to 2 March 2026). Tumor volume doubling time $Td = [\ln(2) \times \Delta t] / \ln(V6 / V5) = (0.693147 \times 210) / 3.79363 = 38.37$ days (5.47 sequential doublings).

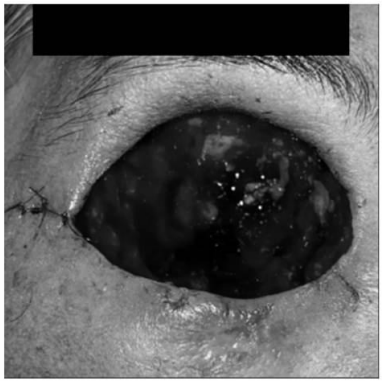
3.3. Radical exenteration, histopathology (T_3), and untreated recurrence (T_4 to T_6)

Because of the massive Stage IIIC (cT4eN0M0) intraorbital tumor burden and the intractable cranial-radiating pain, the patient underwent radical right total orbital exenteration under general anesthesia with orotracheal intubation (GA-OTT) on 30 January 2025 (Epoch T_3, Month 17.5). Antisepsis used 1:9 povidone-iodine, with 360° periorbital subcutaneous infiltration of lidocaine and epinephrine. A circumferential skin incision was made 1 cm beyond the superior and inferior palpable tumor margins. The subcutaneous tissue was undermined down to the bony orbital rim. The periosteum was incised sharply and elevated subperiosteally with a periosteal elevator along all four orbital walls toward the orbital apex. Hemostasis was maintained with careful monopolar and bipolar electrocautery. Exploration confirmed frank osteolytic destruction of the inferior and medial bony orbital walls, so the infiltrated bone was curetted and debrided directly. The residual right optic nerve stump was isolated posteriorly and cross-clamped from the medial and lateral sides with a right-angled clamp. It was transected anterior to the clamp with enucleation scissors, and the orbital contents and adnexa were delivered en bloc (gross specimen dimensions ~4.8 × 4.5 × 4.0 cm). The exenterated bony cavity was packed with gauze impregnated with povidone-iodine and gentamicin. The periorbital skin defect was closed with interrupted 4-0 polypropylene (Prolene) sutures. At the Postoperative Day 8 visit on 7 February 2025, periorbital pain had fallen to NRS 2/10 (a −71.43% reduction from the preoperative NRS 7/10). The Prolene 4-0 skin sutures were intact. There was no active hemorrhage. Mild serous-yellow wound exudate was present, and residual tumor infiltration of the medial bony orbital wall was visible. The BCVA of the contralateral left eye had improved to 6/7.5, with an IOP of 12 mmHg. Histopathologic examination of the exenteration specimen, reported on 10 February 2025, confirmed ocular malignant melanoma with tumor-positive surgical resection margins (reported as R1/R2 at the osteo-periosteal interface). Microscopy at 400× magnification on H&E staining showed diffuse sheets of malignant round-to-ovoid epithelioid melanocytes. The cells had abundant eosinophilic cytoplasm, eccentric nuclei with irregular nuclear membranes, a high N/C ratio, severe nuclear pleomorphism and coarse vesicular chromatin. Prominent eosinophilic cherry-red macronucleoli, brisk mitotic activity and scattered intracellular and extracellular brown melanin pigment granules were also seen, as illustrated in Figure 2.

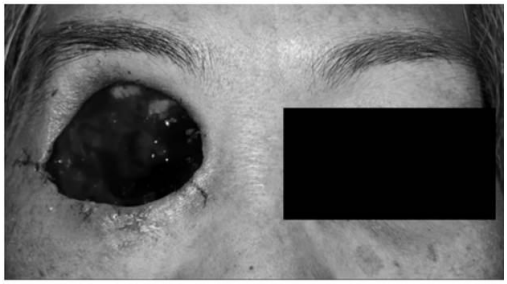
(A) En bloc right orbital exenteration specimen (30 January 2025; centimeter scale)



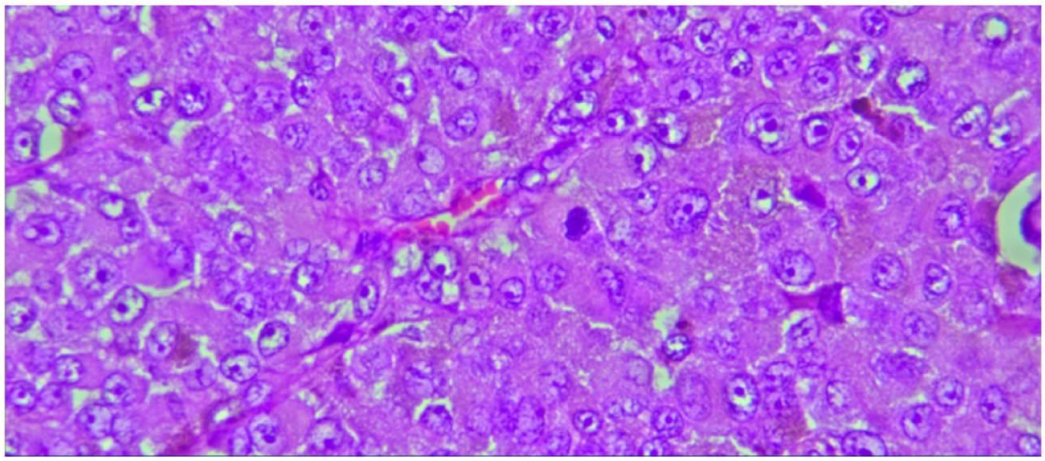
(B) Exenterated socket at POD 8 (7 February 2025): bony wall infiltration



(C) Bilateral periocular view at POD 8 (intact Prolene 4-0 sutures; black bar over OS)



(D) Histopathology of the exenteration specimen (H&E, 400×, 10 February 2025): pleomorphic epithelioid melanocytes, cherry-red macronucleoli, and mitotic figures



(E) Surgical and histopathologic summary (T_3)

1. Intraoperative surgical findings (30 January 2025)

- Procedure: total right orbital exenteration under GA-OTT
- Incision: 360° periorbital, 1.0 cm beyond the tumor margins
- Osteolysis: frank destruction of the inferior and medial orbital walls, requiring periosteal and bony debridement

2. Microscopic pathology (10 February 2025; H&E, 400×)

- Subtype: ocular malignant melanoma (epithelioid): round-to-ovoid cells, abundant eosinophilic cytoplasm, eccentric nuclei, irregular nuclear membranes
- Nuclear features: high N/C ratio, severe pleomorphism, vesicular chromatin, prominent cherry-red macronucleoli
- Proliferation and pigment: frequent mitotic figures with intracellular and cytoplasmic brown melanin granules
- Resection margins: tumor-positive (R1/R2 osteo-periosteal bed), indicating high local relapse risk

Figure 2. Radical right orbital exenteration (T_3, 30 January 2025), postoperative Day 8 socket (7 February 2025), and histopathology (10 February 2025, H&E, 400×): (A) en bloc exenteration specimen with centimeter scale; (B, C) socket at postoperative Day 8 with intact lateral Prolene 4-0 skin sutures and residual medial and inferior bony wall tumor infiltration; (D) photomicrograph showing sheets of round-to-ovoid epithelioid melanocytes, abundant eosinophilic cytoplasm, eccentric vesicular nuclei, prominent cherry-red macronucleoli, frequent mitotic figures, and melanin pigment granules; (E) summary of surgical findings and pathology, with margin positivity (reported as R1/R2). Facial features are masked with black bars (ICMJE/COPE).

The margins were tumor-positive (R1/R2) at the osteo-periosteal interface and the histology was high-grade epithelioid. The patient was therefore referred at once to the Medical Hemato-Oncology (HOM) Division. The plan was systemic adjuvant chemotherapy with intravenous dacarbazine (DTIC), after pre-chemotherapy echocardiography, abdominal ultrasonography and hepatorenal laboratory clearance, together with immunohistochemical (IHC) molecular profiling. She refused both IHC testing and adjuvant chemotherapy. She asked to be transferred back to the secondary regional hospital for local wound dressing. At the 6-week post-exenteration evaluation on 11 March 2025 (Epoch T_4, Month 18.5), the exenterated right socket showed minor purulent seepage on the gauze tamponade and persistent tumor infiltration of the bony walls. The left eye remained stable (BCVA 6/9.5 PHNI, IOP 10 mmHg). She again declined systemic therapy and stayed away from tertiary oncology care for the next 5 months. On 4 August 2025 (Epoch T_5, Month 24.0; 6 months after exenteration), she returned to the ROO clinic. A recurrent, firm, non-tender solid mass lay on the medial side of the right exenterated socket. It measured 2.50 × 1.50 × 1.50 cm (ellipsoid volume V_5 = 2.95 cm^3). Surface crusting and mucopurulent exudate covered it and hid the underlying bony defect (left eye BCVA 6/9.5 PHNI, IOP 11 mmHg). Multiparametric contrast-enhanced head and orbital MRI on 14 August 2025 confirmed multifocal heterogeneous solid recurrent masses in the medial right orbital surgical bed (rT4eN0M0, Recurrent Stage IIIC). The tumor extended directly into the right ethmoid and right frontal paranasal

sinuses. It infiltrated the greater wing of the right sphenoid bone, the right frontal bone and the right nasal bone, and it had completely destroyed the right lamina papyracea and right ethmoid air cells. The MRI also showed incidental small-vessel ischemic changes (Fazekas Grade I) in the deep white matter of both parietal lobes, the centrum semiovale and the corona radiata, and a left maxillary sinus retention cyst. She was urgently counseled to start salvage dacarbazine chemotherapy. She delayed and refused it. Systemic therapy was postponed for a further 7.0 consecutive months (September 2025 to March 2026; 210 days) because of rural travel distance, out-of-pocket accommodation costs and family socioeconomic constraints. In March 2026 (Epoch T_6, Month 31.0; 13.5 months after exenteration) she returned with a massive, fungating, exophytic right craniofacial tumor measuring 6.50 × 7.00 × 5.50 cm (ellipsoid volume V_6 = 131.03 cm^3). The skin over it was hyperemic, excoriated and ulcerated, and she had right facial paresthesia along the ophthalmic and maxillary trigeminal nerve distributions (CN V1/V2), together with two newly palpable, mobile, non-tender right inferoauricular lymph nodes measuring 1.00 × 2.00 × 1.00 cm (V = 1.05 cm^3) and 1.00 × 1.00 × 1.00 cm (V = 0.52 cm^3; total nodal volume 1.57 cm^3; cN1). Figure 3 illustrates these findings.

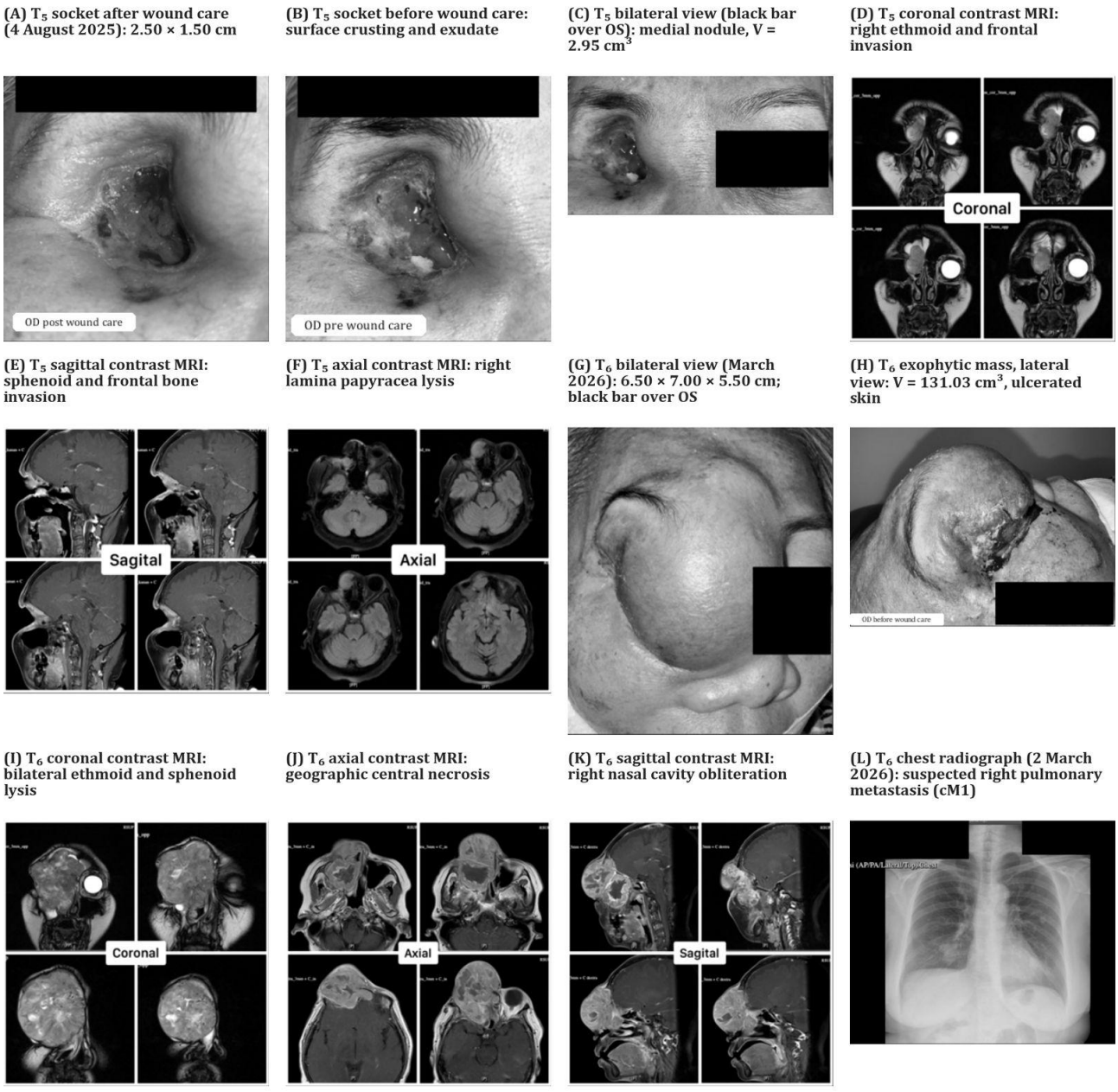


Figure 3. Clinical and radiologic progression after exenteration (T_5 to T_6) without chemotherapy: (A, B) medial socket recurrence at T_5 (4 August 2025; 2.50 × 1.50 × 1.50 cm, V = 2.95 cm^3) after and before wound care; (C) bilateral view at T_5; (D–F) coronal, sagittal, and axial contrast MRI (14 August 2025) showing right ethmoid and frontal sinus, sphenoid greater wing, frontal and nasal bone, and lamina papyracea invasion (rT4eN0M0); (G, H) exophytic ulcerated tumor at T_6 (March 2026; 6.50 × 7.00 × 5.50 cm, V = 131.03 cm^3) after a 7-month interval without therapy; (I–K) coronal, axial, and sagittal contrast MRI (12 March 2026) showing central necrosis, bilateral lamina papyracea and ethmoid/sphenoid sinus destruction, right nasal cavity obliteration, and leftward septal shift; (L) chest radiograph (2 March 2026) raising suspicion of right pulmonary metastasis (Stage IV, cT4eN1M1). Facial features are masked with black bars (ICMJE/COPE). PACS headers are masked.

3.4. Craniofacial progression, Stage IV disease, and growth kinetics (T_6)

Repeat multiparametric contrast-enhanced head and orbital MRI on 12 March 2026 (Epoch T_6) showed trans-midline craniofacial progression. The 131.03 cm^3 heterogeneous solid orbital mass now had extensive central geographic necrosis. The lamina papyracea was destroyed bilaterally, as were the sphenoid sinus walls (right-predominant). Both ethmoid labyrinths were invaded (right-predominant). The right nasal cavity was completely obliterated, the right middle and inferior nasal turbinates were infiltrated directly and the

nasal septum was deviated to the left. There was no cerebral parenchymal metastasis or transtentorial herniation. Posteroanterior chest radiography on 2 March 2026 showed progression of the right pulmonary parenchymal nodule, raising suspicion of pulmonary metastasis (cM1; no CT or biopsy confirmation is reported). Thoracic vertebral osteolysis was absent. Serum hepatorenal biochemistry was normal. AST/SGOT and ALT/SGPT were within the institutional reference limits (< 31.0 U/L and < 34.0 U/L, respectively), as were blood urea nitrogen and serum creatinine. The contralateral left eye kept stable visual function (BCVA 6/9.5 PHNI, IOP 11 mmHg). The variation of ±9.09% was well below the 20.0% analytical Reference Change Value threshold. Regional inferoauricular lymphatic metastasis (cN1) and distant pulmonary metastasis (cM1) had now appeared. They upstaged the patient from Recurrent Stage IIIC (rT4eN0M0) to AJCC 8th edition Clinical Stage IV (cT4eN1M1), as detailed in Table 3.

Table 3. Craniofacial imaging, sinonasal and skull-base invasion, contralateral eye, and organ function across disease progression.

Anatomical / Physiological Domain	Diagnostic Parameter	T_2 Pre-Exenteration Baseline (Dec 2024 – Jan 2025)	T_5 6-Month Post-Exenteration Relapse (Aug 2025)	T_6 13.5-Month Massive Progression (Mar 2026)	Clinical & Pathophysiological Interpretation
Right Orbital Cavity & Neurovascular Structures	Contrast CT / Multiparametric MRI Signal & Invasion	Lobulated solid mass (4.80 × 4.60 × 4.20 cm) replacing right globe; direct infiltration of right optic nerve & EOMs	Multifocal heterogeneous solid masses in medial right orbital surgical bed after exenteration	Massive heterogeneous solid tumor (6.50 × 7.00 × 5.50 cm) with central geographic necrosis filling right orbit	Central necrosis at T_6 may reflect rapid volumetric expansion (131.03 cm^3) outstripping vascular supply
Medial Orbital Wall & Ethmoid Complex	Lamina Papyracea & Ethmoid Air Cells	Right medial orbital wall erosion & ipsilateral ethmoid sinus extension	Complete destruction of right lamina papyracea & invasion of right ethmoid air cells	Bilateral lamina papyracea destruction & bilateral ethmoid sinus invasion (right-predominant)	Trans-midline osteolytic progression across the ethmoid labyrinth during 7-month therapy refusal
Frontal, Sphenoid & Nasal Osteology	Cranial Vault, Skull Base & Nasal Cavity	Right frontal sinus extension & inferior/medial orbital wall destruction; no intracranial mass	Infiltration of right frontal sinus, greater wing of right sphenoid bone, right frontal & nasal bones	Bilateral sphenoid sinus wall destruction; right nasal cavity obliteration; right middle-inferior turbinate invasion; leftward septal shift	Extensive skull-base (sphenoid greater wing) and sinonasal destruction made salvage surgical resection unsuitable
Trigeminal & Cerebral Parenchymal Status	Cranial Nerve Function & Brain MRI	Severe right orbital pain radiating to ipsilateral head (NRS 7/10); brain parenchyma normal on CT	Non-tender medial nodule; bilateral parietal/centrum semiovale/corona radiata Fazekas Grade I ischemia; left maxillary cyst	Ipsilateral right facial paresthesia/numbness (CN V1/V2 infiltration); no cerebral metastasis, edema, or herniation	Change from nociceptive mass pain to trigeminal sensory symptoms (CN V1/V2 territory), possibly from perineural infiltration
Regional Lymphatic Basin	Cervical & Peri-auricular Nodes	No palpable cervical or pre-/inferoauricular lymphadenopathy (cN0)	No palpable regional lymphadenopathy (cN0)	Two mobile, non-tender right inferoauricular lymph nodes (1.00 × 2.00 × 1.00 cm & 1.00 × 1.00 × 1.00 cm; cN1)	Regional nodes appeared after cutaneous/adnexal and sinonasal mucosal involvement
Thoracic & Pulmonary Surveillance	Posteroanterior (PA) Chest Radiograph	Aortosclerosis, thoracic spondylosis, indeterminate solitary nodule in right lower lung zone (cM0)	Patient refused interval thoracic staging radiograph	Progressive right pulmonary nodule highly suspicious for pulmonary metastasis (cM1); no thoracic bone lysis	A right lower lung nodule enlarged over 14 months on plain radiographs, suspicious for pulmonary metastasis (no CT or biopsy confirmation reported)
Hepatic & Renal Biochemical Profile	Serum AST (SGOT), ALT (SGPT), BUN & Creatinine	Within normal institutional limits (AST < 31.0 U/L, ALT < 34.0 U/L, Creatinine 0.6–1.1 mg/dL); cleared for GA-OTT	Refused pre-chemotherapy biochemical and abdominal US workup	AST, ALT, ureum, and creatinine within normal reference limits; no clinical jaundice or hepatomegaly	Preserved hepatorenal reserve permitted safe administration of Cycle 1 palliative IV Dacarbazine
Contralateral Left Eye (OS) Integrity	BCVA, IOP (mmHg) & Slit-Lamp Biomicroscopy	BCVA 6/9.5 PHNI; IOP 11 mmHg (T_3 POD 8: BCVA 6/7.5, IOP 12 mmHg); flat bleb; PI (+); PCIOL stable	BCVA 6/9.5 PHNI; IOP 11 mmHg (T_4: IOP 10 mmHg); quiet anterior segment; normal fundus	BCVA 6/9.5 PHNI; IOP 11 mmHg; clear cornea; deep AC; PI (+) at 11 o'clock; PCIOL stable	Complete preservation of contralateral vision & IOP stability (< 20% RCV threshold) across 31.5 months

Abbreviations: AC, anterior chamber; ALT, alanine aminotransferase; AST, aspartate aminotransferase; BCVA, best-corrected visual acuity; BUN, blood urea nitrogen; CN, cranial nerve; CT, computed tomography; EOM, extraocular muscle; GA-OTT, general anesthesia with orotracheal tube; IOP, intraocular pressure; MRI, magnetic resonance imaging; NRS, Numerical Rating Scale; OS, oculus sinister; PA, posteroanterior; PCIOL, posterior chamber intraocular lens; PHNI, pinhole no improvement; PI, peripheral iridectomy; POD, postoperative day; RCV, Reference Change Value; US, ultrasonography.

Over the 210-day untreated recurrence window between T_5 (4 August 2025, V_5 = 2.95 cm^3) and T_6 (2 March 2026, V_6 = 131.03 cm^3), the tumor volume rose by Δ% = +4,341.69%. This is a 44.42-fold increase. The absolute gain was ΔV = +128.08 cm^3 (+0.61 cm^3/day). Relative to the clinical volume at initial tertiary referral (T_2, 23.56 cm^3) and the pre-exenteration CT volume (T_2, 48.56 cm^3), the T_6 recurrence represented net increases of Δ% = +456.15% (5.56-fold) and Δ% = +169.83% (2.70-fold), respectively. During the 210-day hiatus in therapy the specific growth rate was SGR = [ln(131.03 / 2.95) / 210] × 100% = 1.81%/day (instantaneous growth constant k = 0.0181 day^{-1}). The tumor volume doubling time was Td = [ln(2) × 210] / ln(131.03 / 2.95) = 38.37 days (5.47 sequential volume doublings during the 7-month hiatus). The linear tumor dimensions reached 3.68 × limit for basal diameter (70.0 mm vs 19.0 mm COMS limit) and 5.50 × limit for thickness (55.0 mm vs 10.0 mm COMS limit), as illustrated in Figure 4.

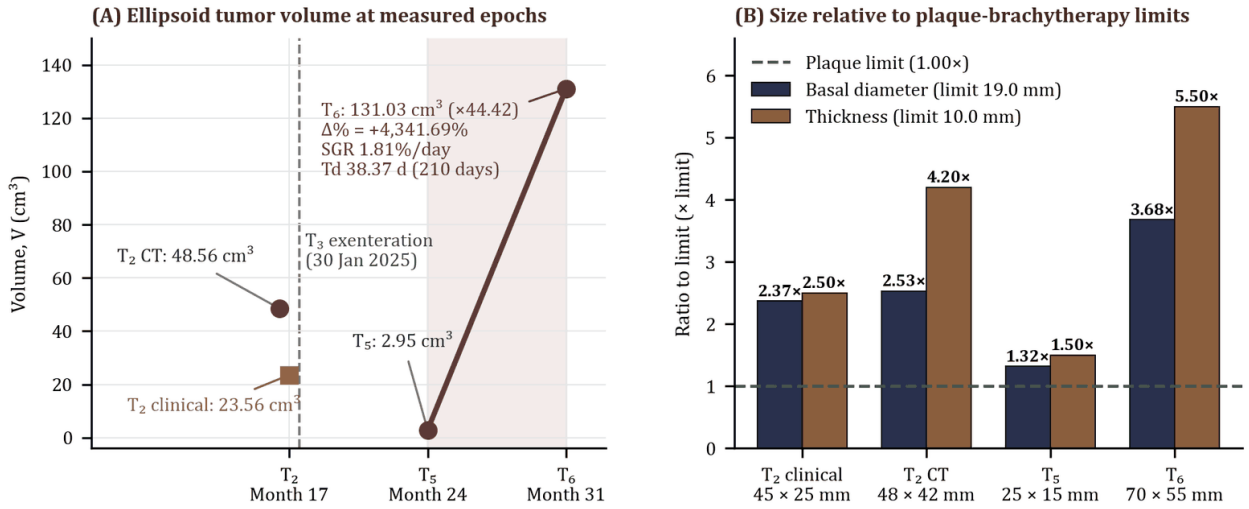


Figure 4. Tumor volume and size relative to plaque-brachytherapy limits (n = 1): (A) ellipsoid volume (V = [π/6] × L × W × H, cm^3) at T_2, T_5, and T_6, with the T_2 clinical caliper volume (23.56 cm^3) shown separately; over the 210-day untreated interval the volume rose 44.42-fold (Δ% = +4,341.69%), SGR = 1.81%/day, Td = 38.37 days; volumes at T_0, T_1 and T_3 are not shown because they are not reported; (B) basal diameter and thickness ratios (× limit) relative to the plaque-brachytherapy limits (≤ 19.0 mm basal diameter, ≤ 10.0 mm thickness).

3.5. Single-cycle palliative dacarbazine (T_7) and literature comparison

In late March 2026 (Epoch T_7, Month 31.5) the patient was re-staged by the multidisciplinary team as having Stage IV (cT4eN1M1) orbital malignant melanoma. The Medical Hemato-Oncology Division then began a planned 3-cycle regimen of intravenous dacarbazine (DTIC) at 4-week intervals. She received Cycle 1 without acute hypersensitivity, severe myelosuppression or drug-induced hepatorenal decompensation. Immediately afterward, she and her family chose to stop further chemotherapy at Prof. Dr. I.G.N.G. Ngoerah General Hospital. The financial burden of inter-regency transportation and urban accommodation in Denpasar was prohibitive. They asked for formal transfer of care to the palliative medicine unit at Tabanan Regional Hospital (RSUD Tabanan). At last follow-up in late March 2026 she was ambulatory (Eastern Cooperative Oncology Group [ECOG] performance status 1) and still did light daily agricultural work. Intermittent mild craniofacial discomfort was controlled by oral analgesics. The sequence was as follows: evisceration without histology (T_0), tumor-positive exenteration margins with refusal of adjuvant therapy (T_3), recurrence 6 months later (T_5) and Stage IV disease after a further 7 months without treatment (T_6). These events are associated in time; the report cannot separate their individual contributions. The neglect consisted of iatrogenic scleral disruption at T_0 and 19.0 cumulative months of refusal of systemic therapy (6 months after T_1 plus 13 months after T_3). For Cycle 1 dacarbazine, the Naranjo ADR Probability Scale gave a total score of 0 (Doubtful/Absent severe drug toxicity) and the WHO-UMC causality framework gave the category Unlikely. Stopping treatment at T_7 therefore resulted from socioeconomic and geographic barriers and not from chemotherapy-induced organ toxicity, as detailed in Table 4.

Table 4. Sequence of care events and intervals, and Naranjo/WHO-UMC assessment of dacarbazine Cycle 1.

Event or interval	Documented evidence	Quantitative anchor	Note
Temporal sequence	Inadvertent evisceration (T_0, Aug 2023) preceded socket recurrence (T_1, Jun 2024) by 10 months; tumor-positive exenteration and refusal of adjuvant therapy (T_3, Feb 2025) preceded recurrence (T_5, Aug 2025) by 6 months and Stage IV progression (T_6, Mar 2026) by 13 months	T_0 (0 mo) → T_1 (10 mo) → T_2 (17 mo) → T_3 (17.5 mo) → T_5 (24 mo) → T_6 (31 mo)	The events are associated in time; their individual contributions cannot be separated in one patient
Volume change over the untreated interval	The 7-month untreated interval (T_5→T_6) was followed by an increase from 2.95 cm^3 to 131.03 cm^3	Δ% = +4,341.69% (T_5→T_6); +456.15% vs the T_2 clinical volume (23.56 cm^3)	Volumes derive from the dimensions recorded at the clinical visits (Table 2)
Interval without adjuvant therapy and stage	6-month delay (T_1→T_2): 48.56 cm^3, Stage IIIC; 13 months after exenteration (T_3→T_6): 131.03 cm^3 with cN1 and cM1	Delay 6 mo → V = 48.56 cm^3 (cT4eN0M0); 13 mo → V = 131.03 cm^3 (cT4eN1M1)	Two intervals, each with a different disease state
Histopathology	Exenteration specimen (400× H&E): epithelioid morphology, increased N/C ratio, cherry-red nucleoli, frequent mitoses; tumor-positive osteo-periosteal margins	H&E (400×); margin status reported as R1/R2	No immunohistochemistry or molecular testing was done
Naranjo ADR Probability Scale and WHO-UMC (Cycle 1 dacarbazine at T_7)	AST, ALT, BUN and creatinine remained normal after Cycle 1 of IV dacarbazine; mild intermittent pain was tumor-related	Naranjo total score 0 (doubtful); WHO-UMC category: unlikely	Discontinuation after Cycle 1 was attributed to socioeconomic and geographic barriers, not to drug toxicity

Abbreviations: ADR, adverse drug reaction; ALT, alanine aminotransferase; AST, aspartate aminotransferase; BUN, blood urea nitrogen; DTIC, dacarbazine; H&E, hematoxylin and eosin; N/C, nuclear-to-cytoplasmic; WHO-UMC, World Health Organization–Uppsala Monitoring Centre.

To place the clinical course in the context of the ocular oncology literature, the findings were compared with nine international reference cohorts. They covered orbital melanoma, extraocular extension and radical orbital exenteration, and were published between 2021 and 2026.[2,5,10,14,18–22] In these series, primary surgery with inadequate margins or iatrogenic scleral violation consistently led to orbital tumor seeding, and tumor-positive (R1) exenteration margins without immediate postoperative radiotherapy was associated with local relapse and poorer survival in several of these series. Median overall survival was 11.9 months in a series of metastatic ocular and orbital melanoma[20], as detailed in Table 5.

Table 5. Published cohorts of orbital melanoma, extraocular extension, and orbital exenteration (2021–2026) compared with the index case

Author, Year & Study Setting	Study Design & Sample Size (N)	Tumor Subtype, Origin & Staging Profile	Primary Surgical & Adjuvant Modalities	Recurrence, Margin Status & Survival Outcomes	Comparative Alignment With Index Case (Dana et al., 2026)
Huang et al. (2021)[5] Taipei Veterans General Hospital, Taiwan	34-year tertiary referral cohort (N = 88 ocular melanomas)	Uveal (62.5%), conjunctival, eyelid, and orbital melanomas in an East Asian population	Enucleation, orbital exenteration, local excision, radiotherapy, and systemic chemotherapy	2-year recurrence rate after surgery was 38.0% for orbital melanoma vs 4.0% (5-yr) for uveal and 6.0% for conjunctival	Shows higher local relapse propensity of orbital melanoma (38.0%) in Asian populations
Baum et al. (2022)[19] University Hospital Essen, Germany	Retrospective tertiary exenteration cohort (N = 76: 60 CoM, 16 UM)	Advanced conjunctival (CoM) and extrascleral uveal melanoma (UM) requiring orbital exenteration	Total or subtotal orbital exenteration ± adjuvant radiotherapy or systemic chemotherapy	1-yr OS 82%, 5-yr OS 52%; lymph node metastasis, distant metastasis, R1 margins, and post-exenteration relapse predicted poor OS	Mirrors our patient's adverse prognostic triad: R1/R2 bony margins (T_3), socket relapse (T_5), and nodal/lung metastasis (T_6)
Liu et al. (2023)[20] Fudan & Beijing Bi-Institutional Cohort, China	Bi-institutional retrospective cohort (N = 51 patients with metastatic ocular and orbital melanoma)	Metastatic ocular and orbital melanoma (Stage IV; hepatic, pulmonary, nodal, and bone metastases)	First-line systemic chemotherapy (DTIC-based), targeted therapy, or immune checkpoint blockade	Median overall survival (OS) only 11.9 months; hepatic and pulmonary metastases dominated systemic progression	Contextualizes our patient's transition to Stage IV (cT4eN1M1) with right pulmonary metastasis and limited DTIC efficacy
Zong et al. (2023)[21] Shanghai Ninth People's Hospital, China	Retrospective tertiary cohort (N = 32 exenterations among 79 conjunctival melanoma patients)	Advanced ocular surface and orbital melanoma undergoing orbital exenteration	Orbital exenteration ± adjuvant radiotherapy and systemic therapy	Local recurrence 9.4%, regional nodal metastasis 18.8%, distant metastasis 50.0%, disease-specific mortality 46.9%	Demonstrates high distant and regional nodal dissemination rates once melanoma invades orbital soft tissues
Qedair et al. (2023)[22] MD Anderson & Multicenter Meta-Analysis, USA	Systematic review & meta-analysis (33 articles; 957 patients)	Advanced craniofacial and orbital malignancies invading the bony orbit and paranasal sinuses	Total or extended orbital exenteration with skull-base/sinonasal bony resection ± adjuvant RT	Positive surgical margins and sinonasal/skull-base bony invasion significantly reduced disease-free and overall survival	Resembles our patient's medial/inferior orbital wall osteolysis at T_3 and bilateral sinonasal invasion at T_5–T_6
Li et al. (2025)[2] Beijing Tongren Hospital, China	Retrospective single-center cohort (N = 37 orbital melanomas)	Secondary (89.2%: 32.4% CoM, 29.7% UM, 21.6% eyelid, 5.4% lacrimal) & primary (10.8%) orbital melanoma; 70.3% female; mean age 55 yr	Orbital exenteration or wide excision integrated with systemic adjuvant therapy and radiotherapy	Optic nerve invasion and incomplete systemic integration independently predicted worse survival; female predominance (70.3%)	Similar age and sex (56-yr Asian female) and similar anatomic involvement (optic nerve and EOM invasion at T_2)
Niinimäki et al. (2025)[18] Helsinki University Hospital, Finland	Retrospective tertiary cohort (N = 69 exenterations)	Orbital and periorbital malignancies (uveal melanoma most frequent at 14%, followed by BCC and cSCC)	Radical orbital exenteration and reconstructive surgery evaluated by multidisciplinary tumor board	1-yr DFS 74%, 2-yr DFS 67%; exenteration could have been avoided in 46% (32/69) if primary surgery had sufficient margins without delay	Suggests that primary surgical inadequacy (T_0 evisceration, T_1 semi-enucleation) and treatment delay drive salvage exenteration failure
Gentile et al. (2026)[10] Hospital Italiano Buenos Aires, Argentina	Observational analytical cohort (N = 181 UM; 12 EOE)	Uveal melanoma with extrascleral orbital extension (EOE, 6.62%; mean age 64.4 yr)	Enucleation, orbital exenteration, or plaque brachytherapy with long-term systemic surveillance	EOE occurred in larger tumors (mean basal diameter 17.7 mm) and strongly predicted early systemic metastasis within 12 months	Suggests how breach of the scleral barrier (via T_0 evisceration and T4e extension) accelerates orbital and pulmonary spread
Chetroiu et al. (2026)[14] Leiden University Medical Center, Netherlands	Retrospective referral-centre cohort (N = 27 exenterations for conjunctival melanoma)	Conjunctival melanoma undergoing orbital exenteration	Orbital exenteration ± postoperative radiotherapy and systemic targeted/immunotherapy	1-yr OS 92%, 5-yr OS 57%; distant metastasis in 26%; tumor-containing resection margins were related to worse progression-free survival at 5 years	Suggests that R1/R2 osteo-periosteal margins require immediate postoperative radiotherapy/systemic therapy to prevent massive relapse
Index Study (2026) RSUP Prof. Dr. I.G.N.G. Ngoerah, Bali, Indonesia	Case report (N = 1; 8 epochs, 31.5 mo)	56-yr female farmer; neglected recurrent orbital melanoma post-inadvertent evisceration; Stage IIIC (cT4eN0M0) → Stage IV (cT4eN1M1)	Inadvertent evisceration (T_0) → semi-enucleation (T_1) → radical exenteration (T_3, R1/R2) → 13-mo refusal → 1 cycle DTIC (T_7) → palliative care	44.42-fold volumetric expansion (2.95 → 131.03 cm^3; Td = 38.37 days) with bilateral sinonasal/skull-base destruction & cN1M1 dissemination	Descriptive two-point volumetric growth estimate (SGR, Td) in a neglected orbital melanoma in an LMIC agricultural setting

Abbreviations: BCC, basal cell carcinoma; CoM, conjunctival melanoma; cSCC, cutaneous squamous cell carcinoma; DFS, disease-free survival; DTIC, dacarbazine; EOE, extrascleral/extraocular extension; LMIC, low- and middle-income country; OS, overall survival; RT, radiotherapy; SGR, specific growth rate; Td, tumor volume doubling time; UM, uveal melanoma. Sample sizes are as given in the registered abstracts of the cited articles.

4. Discussion

4.1. Two-stage clinical neglect in orbital melanoma

The clinical, radiologic and histopathologic course documented here illustrates how two-stage clinical neglect may be followed by progression of an intraocular or orbital melanoma to a massive, trans-midline Stage IV (cT4eN1M1) craniofacial malignancy. The first stage was an inadvertent ocular evisceration at a secondary hospital, and the second was repeated socioeconomic refusal of adjuvant therapy after radical orbital exenteration. Orbital malignant melanoma occupies a particularly lethal niche in ophthalmic oncology. The bony orbit lacks internal lymphatic septa posteriorly. Even so, it communicates directly with the middle cranial fossa through the optic canal and superior orbital fissure. It also communicates with the pterygopalatine and infratemporal fossae through the inferior orbital fissure, and with the ethmoid, frontal and maxillary paranasal sinuses across the paper-thin lamina papyracea and orbital floor. Once malignant melanocytes breach the dense collagenous barrier of the sclera, they reach the richly vascularized intraconal and extraconal orbital fat pads, the extraocular muscle sheaths and the periosteum (periorbita). Two routes lead there. One is spontaneous extrascleral extension along vortex veins and ciliary neurovascular bundles (AJCC subcategory T4e, > 5.0 mm). The other is iatrogenic surgical transection during an unplanned evisceration.

The following framework, drawn from the literature and not from measurements in this patient, outlines five tiers that may be relevant: occupational environmental carcinogenesis, molecular and cytogenetic oncogenesis, iatrogenic surgical seeding, exponential osteolytic regrowth, and late lymphatic and hematogenous dissemination, as illustrated in Figure 5.

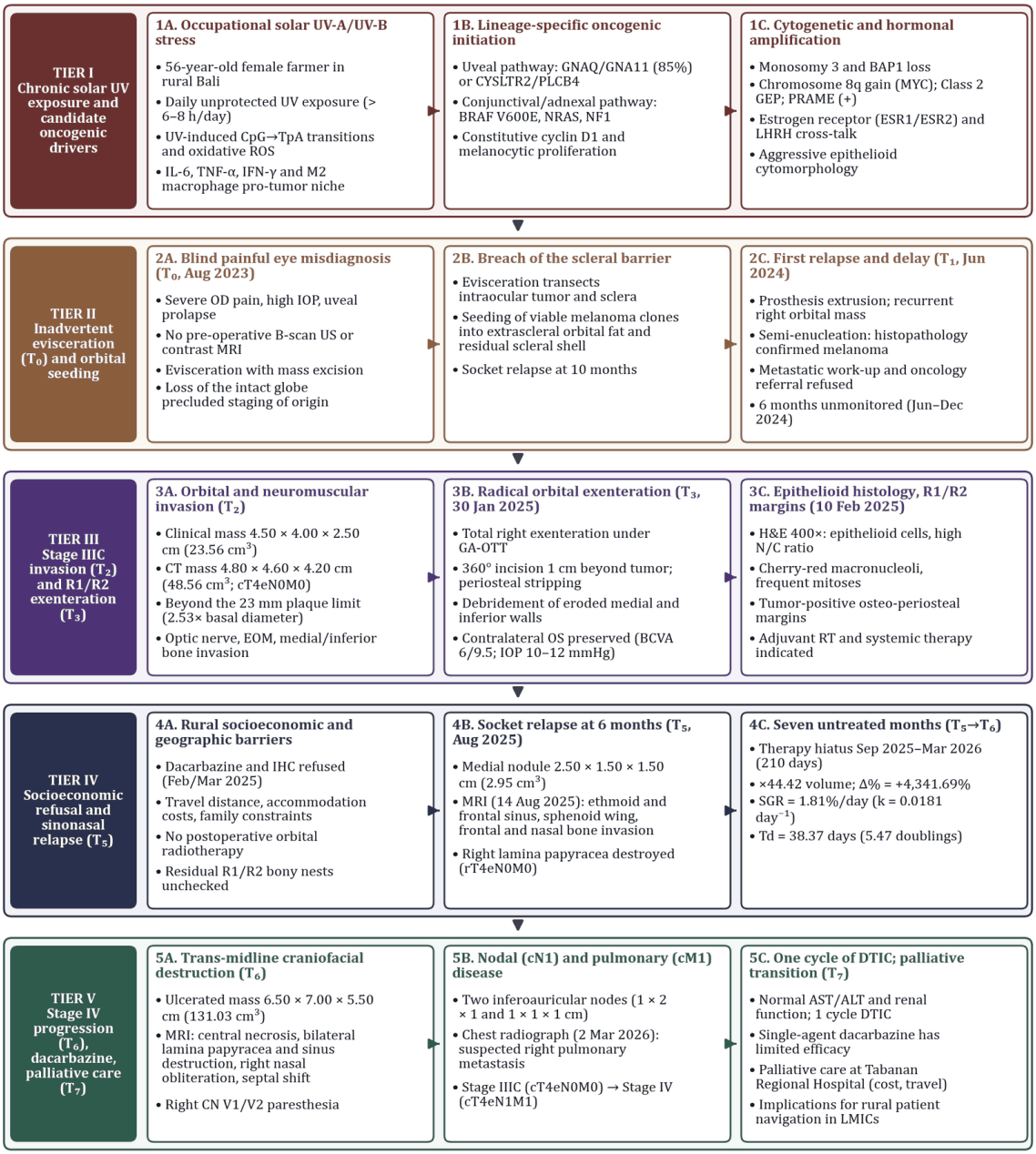


Figure 5. Proposed five-tier framework for the course in this patient, drawn from the literature and not from measurements in this patient: Tier I, chronic occupational solar UV exposure and candidate oncogenic drivers (GNAQ/GNA11, BRAF/NRAS, BAP1 loss, monosomy 3, 8q gain); Tier II, scleral disruption at inadvertent evisceration (T_0, August 2023); Tier III, Stage IIIC orbital invasion (T_2) and tumor-positive radical exenteration with epithelioid histology (T_3); Tier IV, socioeconomic refusal of chemotherapy and untreated sinonasal recurrence (T_5 to T_6; SGR = 1.81%/day, Td = 38.37 days); Tier V, skull-base destruction, nodal (cN1) and suspected pulmonary (cM1) Stage IV disease, single-cycle dacarbazine, and palliative care (T_7, March 2026).

4.2. Ultraviolet exposure, evisceration, surgical margins, and systemic therapy

The age and occupational profile of this 56-year-old female agricultural worker resembles recent Asian orbital melanoma cohorts. It may also reflect sex-specific and environmental mechanisms. Large Western and Japanese registry studies of conventional intraocular uveal melanoma show a balanced sex distribution and a median age in the seventh decade at diagnosis. The prospective Collaborative Ocular Oncology Group Study No. 2 (COOG2) enrolled 1,577 patients (51.3% male, median age 64.0 years),[23] and the Japanese National Comprehensive Genome Profiling database included 569 patients (51.1% male, median age 66.0 years).[24] Primary and secondary orbital melanomas begin earlier. In the Beijing Tongren Hospital cohort reported by Li et al.[2], the mean age was 55.0 years (range 28–75 years) and 70.3% of patients were female (26 females vs 11 males). This patient's age at tertiary referral (56 years) is close to that mean. Translational studies also suggest that female sex hormones and reproductive history modulate ocular melanoma biology, and the proposed route is through estrogen receptors (ERα/ESR1 and ERβ/ESR2) and luteinizing hormone-releasing hormone (LHRH) receptors in the tumor microenvironment.[25] Immunohistochemical and The Cancer Genome Atlas (TCGA) transcriptomic analyses have shown ER positivity in about 60.0% of uveal melanomas. ESR1 and ESR2 expression is higher in a subset of tumors with poor genetic prognostic features, such as monosomy 3 and somatic BRCA1-associated protein-1 (BAP1) loss.[26]

The patient also had three decades of occupational exposure to intense equatorial solar ultraviolet (UV) radiation during daily farm work in Bali. Cutaneous melanoma is classically driven by UV-induced cyclobutane pyrimidine dimers (C>T transitions at dipyrimidine sites). These affect BRAF V600E, NRAS and NF1. In ocular and orbital melanoma, chronic solar UV exposure acts in two ways. It causes direct mutagenesis of the anterior segment and conjunctiva, and it remodels the microenvironment indirectly through photo-oxidation.[27,28] A systematic review of meta-analyses reports odds ratios of 1.64 for propensity to sunburn, 1.80 for fair skin color and 1.75 for light eye color, whereas occupational sunlight exposure was not a significant factor.[29] At the molecular level, Orozco et al. validated an ultraviolet light response gene signature in uveal melanoma. Chronic UV-induced reactive oxygen species (ROS) and CpG-to-TpA transitions at activating hotspots in GNAQ, GNA11 and RAC1 sustain upregulation of interleukin-6 (IL-6), tumor necrosis factor-alpha (TNF-α), interferon-gamma (IFN-γ) and CC/CXC chemokines. This photo-inflammatory cascade recruits tumor-associated M2 macrophages, dendritic cells and plasma cells. It fosters neoangiogenesis and local T-cell exhaustion.

The first major turning point in the patient's course was the inadvertent ocular evisceration in August 2023 (Epoch T_0). The painful, hypertensive right eye had been misdiagnosed as bulbar prolapse. Evisceration of an eye with an occult malignant melanoma is a serious surgical pitfall worldwide. It is preventable.[11] Necrotic or advanced uveal melanomas often cause secondary angle-closure or neovascular glaucoma, total exudative retinal detachment and intraocular hemorrhage, and they can also cause sterile panophthalmitis or orbital cellulitis driven by tumor necrosis, so the eye presents as blind and acutely painful, with opaque media or uveal staphyloma/prolapse. If evisceration is done without prior B-mode ultrasonography or contrast-enhanced MRI, the surgeon incises the corneoscleral limbus and curettes friable intraocular tumor, which can seed viable malignant melanocytes into the extrascleral Tenon capsule and orbital fat while a scleral shell, whose emissary canals often hold microscopic tumor cords, stays inside the orbit. Destruction of the intact globe at T_0 also prevented any later pathologic determination of the tumor's origin. It could have been a primary posterior uveal melanoma with extrascleral extension, or a primary conjunctival or adnexal melanoma invading the globe. According to NCCN (Version 2.2026) and UK national guidelines, any blind, painful eye with opaque media must have B-scan ultrasonography or contrast-enhanced orbital MRI, or both, before globe-destructive surgery. When melanoma is found after an inadvertent evisceration, immediate secondary enucleation of the residual scleral shell is required. Orbital radiotherapy or exenteration follows.

A second factor associated with the poor outcome was the combination of tumor-positive (R1/R2) bony resection margins at radical orbital exenteration (Epoch T_3) with 19.0 cumulative months of patient-driven refusal of treatment. These were 6 months after the T_1 semi-enucleation and 13 months after the T_3 exenteration. At T_2, the 4.80 × 4.60 × 4.20 cm (48.56 cm^3) orbital mass was 2.53-fold wider and 4.20-fold thicker than the maximum COMS plaque brachytherapy limits (≤ 19.0 mm basal diameter and ≤ 10.0 mm thickness for a 23.0 mm plaque).[17] It infiltrated the optic nerve, extraocular muscles and medial and inferior orbital walls. Conservative radiotherapy was therefore impossible. Radical orbital exenteration was needed. International oculoplastic series report better disease-free survival with primary exenteration plus adjuvant radiotherapy than with wide local excision.[8] Niinimäki et al. found that 46.0% (32/69) of orbital exenterations could have been avoided if primary surgery had achieved clear margins without delay.[18] In this patient, exenteration at T_3 debulked the 48.56 cm^3 mass and relieved cranial pain by −71.43%. However, the tumor had already eroded the medial and inferior orbital walls. Histopathology on 10 February 2025 showed tumor-positive (R1/R2) osteo-periosteal margins populated by sheets of epithelioid melanocytes with prominent cherry-red macronucleoli and brisk mitoses. In the cohorts compared in Table 5, tumor-containing resection margins were related to worse progression-free survival at 5 years,[14] and 5-year overall survival after exenteration was 52% to 57%.[14,19] Without adjuvant therapy, the residual microscopic tumor of this patient reappeared at 6 months (T_5) as a 2.95 cm^3 medial socket nodule. It then grew 44.42-fold (Δ% = +4,341.69%) over 210 untreated days to 131.03 cm^3 (T_6). The exponential Specific Growth Rate was 1.81%/day and the Tumor Volume Doubling Time 38.37 days.

The change in stage from Stage IIIC (cT4eN0M0 at T_2 and rT4eN0M0 at T_5) to Clinical Stage IV (cT4eN1M1 at T_6) illustrates an important principle of the AJCC 8th edition classification.[30] The intraocular uveal tract has no lymphatic vessels. Confined intraocular uveal melanomas therefore spread almost exclusively through the blood. They cause hepatic metastases in up to 90.0% of metastatic patients and pulmonary metastases in 16%. They almost never metastasize to regional lymph nodes.[7,30] The situation changes once melanoma invades the extrascleral orbital soft tissues, palpebral conjunctiva, periocular skin or sinonasal mucosa. In this patient that meant the right ethmoid, frontal and sphenoid sinuses and the middle and inferior nasal turbinates at T_5–T_6. Tumor cells can then enter the superficial and deep craniofacial lymphatic plexuses that drain toward the preauricular, parotid, inferoauricular and submandibular lymph nodes.[30–32] The two mobile right inferoauricular lymph nodes (1.00 × 2.00 × 1.00 cm and 1.00 × 1.00 × 1.00 cm; total volume 1.57 cm^3; cN1) and the progression of the right pulmonary nodule (cM1) at T_6 reflected invasion beyond the orbit. They upstaged the disease to Stage IV. After metastasis, median overall survival is about 10 to 13 months[33] (11.9 months in one series of metastatic ocular and orbital melanoma[20]).

The systemic management of this patient also illustrates the gap between current precision oncology and real-world access to drugs in low- and middle-income countries (LMICs). In high-income settings, molecular profiling divides ocular and orbital melanomas into subgroups with targetable alterations. Uveal-origin tumors carry mutually exclusive GNAQ or GNA11 driver mutations (~85.0%) or the rarer CYSLTR2 and PLCB4 alterations,[4,34] and metastatic risk modifiers include BAP1 loss, monosomy 3, chromosome 8q gain, SF3B1, EIF1AX, 15-gene expression profile [15-GEP] Class 2 and PRAME positivity. Conjunctival and cutaneous-origin orbital melanomas often carry BRAF V600E (30.0%–50.0%), NRAS, NF1 or KIT mutations that respond to combined BRAF/MEK inhibition (dabrafenib plus trametinib) or to anti-PD-1/CTLA-4 immune checkpoint blockade (nivolumab plus ipilimumab, or pembrolizumab).[24,35] For HLA-A*02:01-positive metastatic uveal melanoma, the bispecific gp100-targeted T-cell receptor fusion protein tebentafusp is the ASCO and NCCN Category 1 preferred first-

line therapy.[35] It gave a 3-year overall survival of 27.0% versus 18.0% for investigator's choice therapy (hazard ratio 0.68).[36,37] In a small single-arm trial of niraparib in melanoma with homologous recombination pathway alterations, none of the four patients with uveal melanoma responded, although responses occurred in non-uveal melanoma.[38] Single-agent cytotoxic dacarbazine (DTIC) has limited efficacy in metastatic uveal melanoma.[39] In this rural Indonesian setting the patient declined immunohistochemistry and next-generation molecular profiling. Tebentafusp was unavailable. Dacarbazine was the only accessible systemic treatment at T_7. Transport and accommodation costs still forced discontinuation. Only a single cycle was given. This shows the need for subsidized rural patient navigation, tele-oncology wound surveillance and decentralized radiotherapy and systemic treatment access within national cancer control programs.[40]

4.3. Imaging of sinonasal and skull-base invasion

A major radiologic contribution of this study is the serial documentation of trans-compartmental craniofacial bone destruction. It rests on sequential contrast-enhanced CT (Epoch T_2) and multiparametric contrast-enhanced MRI (Epochs T_5 and T_6). In orbital melanoma, high-resolution MRI gives better soft-tissue contrast than CT because it exploits the paramagnetic properties of melanin granules, which shorten T_1 and T_2 relaxation times, so pigmented clones appear hyperintense on T_1-weighted and hypointense on T_2-weighted images. MRI also delineates optic nerve sheath invasion, extraocular muscle replacement and dural or perineural extension.[41,42] At Epoch T_2 (December 2024), the orbital CT showed a 4.80 × 4.60 × 4.20 cm (48.56 cm^3) mass confined mainly to the right orbit, with early medial and inferior wall erosion. The patient then underwent radical orbital exenteration with R1/R2 bony margins (Epoch T_3) and had 6 months of untreated growth. The Epoch T_5 MRI (14 August 2025) showed that residual tumor nests in the medial periosteal bed had breached the right lamina papyracea. This is the thinnest cortical barrier of the medial orbit, only 0.2 to 0.4 mm thick. The tumor had invaded the low-resistance pneumatic spaces of the right ethmoid labyrinth and right frontal sinus. It also infiltrated the greater wing of the right sphenoid bone at the boundary of the middle cranial fossa.

During the 210-day untreated interval between T_5 and T_6 (August 2025 to March 2026), the volume rose from 2.95 cm^3 to 131.03 cm^3 (Δ% = +4,341.69%). The MRI of 12 March 2026 showed two important radiologic and neuro-ophthalmic changes. First, the interior of the 6.50 × 7.00 × 5.50 cm tumor had extensive geographic central necrosis. Central necrosis of this kind is generally attributed to tumor growth that outstrips its oxygen supply (diffusion limit ~150–200 μm from functional neovessels), with intratumoral hypoxia, hypoxia-inducible factor-1α (HIF-1α) upregulation and vascular endothelial growth factor (VEGF)-driven neoangiogenesis as proposed mediators; none of these was measured in this patient.[43] Second, the tumor invaded across the midline through the nasal septum and intersinus septa. It destroyed the contralateral left lamina papyracea and the bilateral sphenoid and ethmoid sinus walls. It obliterated the right nasal cavity completely and infiltrated the right middle and inferior nasal turbinates. This anatomic change coincided with a shift in the main symptom. At T_2 it was severe nociceptive orbital mass pain (NRS 7/10); at T_6 it was ipsilateral facial paresthesia and numbness. The shift may reflect direct perineural infiltration or compressive axonopathy of the ophthalmic (CN V1: supraorbital, supratrochlear and nasociliary/anterior ethmoidal branches) and maxillary (CN V2: infraorbital and pterygopalatine branches) divisions of the trigeminal nerve.

4.4. Histopathology and surgical margins

The high-grade microscopic architecture of the exenteration specimen of 10 February 2025 may account for the rapid regrowth between T_5 and T_6. Under the modified Callender classification and the AJCC 8th edition histopathologic grading framework for ocular melanomas, cell morphology is divided into spindle cell (spindle A and spindle B), mixed cell and epithelioid cell types.[6,16] Spindle cell melanomas consist of cohesive, fusiform cells in tight fascicles with elongated nuclei, indistinct nucleoli, rare mitotic figures and intact intercellular reticulin networks. The prognosis is comparatively favorable. The epithelioid melanocytes that predominated in the exenterated orbital mass of this patient are different. They have large polygonal or round-to-ovoid cell bodies with abundant eosinophilic cytoplasm and have lost E-cadherin-mediated cell-to-cell cohesion. Their nuclear-to-cytoplasmic (N/C) ratios are high, the nuclear membranes are irregular and the chromatin is vesicular. Mitotic activity is brisk, and prominent eosinophilic cherry-red macronucleoli are present.

Prominent cherry-red macronucleoli are the morphologic expression of hyperactive ribosomal RNA (rRNA) transcription and ribosome biogenesis, which have been linked to MYC activity and BAP1 loss in other tumors; neither was tested in this patient.[44,45] Loss of nuclear BAP1 protein disrupts histone H2A deubiquitination (H2AK119ub1). The cells dedifferentiate toward a stem-like, neural crest-progenitor phenotype that resists anoikis. They degrade extracellular matrix and cortical bone through matrix metalloproteinases (MMP-2, MMP-9 and MT1-MMP) and receptor activator of nuclear factor kappa-B ligand (RANKL)-mediated osteoclast activation.[46,47] High-grade epithelioid clones may remain at a tumor-positive (R1/R2) osteo-periosteal margin after exenteration. Wound-healing cytokines such as platelet-derived growth factor (PDGF), transforming growth factor-beta (TGF-β) and epidermal growth factor (EGF) can then stimulate the residual tumor nests.[48] This may help explain why R1 orbital exenterations without immediate postoperative adjuvant radiotherapy (50–60 Gy) show universal rapid local recurrence.

4.5. Health-system considerations

Beyond its cellular and radiologic findings, this case illustrates structural weaknesses in the health system. They turn a localized ocular malignancy that could be controlled into incurable Stage IV craniofacial disease in rural agricultural communities of low- and middle-income countries (LMICs).[40] Two separate bottlenecks compromised the course of this patient. The first was a primary diagnostic failure at the secondary regional hospital (Epoch T_0, August 2023). A blind, painful eye with uveal prolapse underwent evisceration without preoperative B-scan ultrasonography or specialist ophthalmic oncology consultation. The second was a socioeconomic adherence failure at the tertiary referral level (Epochs T_1, T_3, T_4, T_5 and T_7). An under-resourced rural farmer repeatedly declined or stopped metastatic staging, immunohistochemistry, postoperative radiotherapy and multi-cycle dacarbazine chemotherapy. The reasons were inter-regency travel distance and urban accommodation expenses in Denpasar.

Preventing this two-stage cascade needs a coordinated health-policy response with three components across

provincial and national referral networks. First, national ophthalmic surgical guidelines could adopt a "No Evisceration Without Imaging" safety checklist at all secondary hospitals. It would require B-mode ocular ultrasonography and tele-ophthalmology review by a certified ocular oncologist before any evisceration is authorized, with all intraocular surgical specimens submitted for histopathologic examination. Second, tumor-positive (R1/R2) margins or bony orbital wall erosion may be found during orbital exenteration at a tertiary center. Hospital navigation programs should then provide ring-fenced social-welfare housing vouchers and transport subsidies. Rural patients could thus complete a 5-to-6-week course of postoperative fractionated orbital radiotherapy and systemic adjuvant therapy without catastrophic household expenditure. Third, outpatient chemotherapy and structured palliative symptom management should be decentralized to accredited secondary regional hospitals. The shared-care transition between Prof. Dr. I.G.N.G. Ngoerah General Hospital and Tabanan Regional Hospital at Epoch T_7 is an example. Such arrangements let patients with advanced ocular malignancies keep their dignity, pain control and family cohesion in their home communities.[49]

4.6. Limitations

This report has the limits of a single case. The origin of the tumor (primary orbital, uveal, or conjunctival) could not be established because the globe was eviscerated without histology. No immunohistochemical or molecular testing was done, so the diagnosis rests on H&E morphology and the mechanisms discussed above were not tested in this patient. The growth rate and doubling time derive from two volumes obtained on different dates and, in part, by different methods. Distant metastasis was assessed on plain chest radiographs only, and volumes at T_0 and T_1 are not available.

5. Conclusion

In this 31.5-month case report, evisceration without preoperative imaging and prolonged refusal of adjuvant therapy were followed by osteolytic sinonasal recurrence and AJCC 8th edition Stage IV (cT4eN1M1) dissemination of orbital malignant melanoma. Two stages were involved. The first was an inadvertent ocular evisceration without preoperative imaging at a secondary hospital, and the second was 19.0 cumulative months of socioeconomic refusal of systemic adjuvant therapy after a tumor-positive (R1/R2) radical orbital exenteration. Three-dimensional ellipsoid volumetry quantified the regrowth. The orbital tumor expanded 44.42-fold across the 210-day untreated post-exenteration recurrence window (T_5 to T_6). The change was $\Delta\%$ = +4,341.69%, from 2.95 cm^3 to 131.03 cm^3, with an exponential Specific Growth Rate of 1.81%/day and a Tumor Volume Doubling Time of 38.37 days. The result was bilateral destruction of the lamina papyracea and ethmoid-sphenoid sinuses and obliteration of the right nasal cavity. Regional inferoauricular lymphadenopathy (cN1) and pulmonary metastasis (cM1) followed.

Clinically, this case supports two practice recommendations for ophthalmic and oncologic care in resource-limited settings. First, ocular evisceration must be strictly contraindicated in any blind, painful or prolapsed eye until intraocular malignancy has been rigorously excluded, which requires B-scan ultrasonography and contrast-enhanced orbital CT or MRI, and every globe-destructive specimen must undergo histopathologic analysis. Second, patients with high-grade epithelioid histopathology with cherry-red macronucleoli and tumor-positive (R1/R2) osteo-periosteal margins after orbital exenteration need immediate multimodal adjuvant radiotherapy and systemic therapy. Proactive socioeconomic patient navigation, transport subsidies and decentralized rural shared-care oncology networks should support that treatment. The aim is to prevent exponential craniofacial progression and premature mortality.

Declarations

Ethics Approval and Consent to Participate

This case report was reviewed and approved by the CMHC Research Center Ethics Committee, Indonesia (protocol approval number 2026/0418) and followed the Declaration of Helsinki. Written informed consent for surgery, histopathologic examination, serial diagnostic imaging, and systemic chemotherapy was obtained from the patient and her legal family representative.

Consent for Publication

Written informed consent for the publication of anonymized clinical data, longitudinal imaging, histopathologic photomicrographs, and de-identified clinical photographs (black bars over the contralateral ocular and periocular landmarks; PACS headers masked) was obtained from the patient and her legal family representative.

Availability of Data and Materials

All clinical, morphometric, radiologic, histopathologic, and calculated data analyzed in this report are included in the article.

Competing Interests

The authors declare no competing financial, professional, or personal interests that could have influenced the work reported in this article.

Funding

None. This work received no external grant funding from public, commercial, or not-for-profit agencies.

Authors' Contributions

IGNAWKD: Investigation, Data curation, Formal analysis, and Writing – original draft; PY: Conceptualization, Methodology, Supervision, and Writing – review & editing; NMLU: Investigation, Resources, and Validation; IWLA: Investigation, Resources, and Project administration. All authors read and approved the final manuscript.

Acknowledgments

The authors thank the clinical staff of the Reconstructive Oculoplastic and Oncology Division (Department of Ophthalmology), the Medical Hemato-Oncology Division (Department of Internal Medicine), the Department of Radiology, and the Department of Anatomical Pathology at Prof. Dr. I.G.N.G. Ngoerah General Hospital / Faculty of Medicine, Udayana University, Denpasar, Bali, Indonesia, for their multidisciplinary support.

Generative Artificial Intelligence Disclosure

No generative artificial intelligence was used in the study design, data collection, analysis, or interpretation of the findings.

6. References

1. Fernandes JJ, Sharabura AB, Pfannenstiel MM, et al. Metastatic melanoma to the orbit masquerading as idiopathic orbital inflammation: a case report. Front Ophthalmol (Lausanne). 2025;5:1678987. doi: 10.3389/fopht.2025.1678987

2. Li Y, Ma M, Li J, et al. Clinical study of 37 cases of orbital melanoma. BMC Ophthalmol. 2025;25(1):181. doi: 10.1186/s12886-025-03897-0
3. Carter TJ, Broadfoot J, Coupland SE, et al. Uveal melanoma UK national guidelines: 2023 update. Eur J Cancer. 2025;228:115687. doi: 10.1016/j.ejca.2025.115687
4. Iavarone L, Franco R, Zito Marino F, et al. Ocular melanoma: a comprehensive review with a focus on molecular biology. Int J Mol Sci. 2025;26(19):9799. doi: 10.3390/ijms26199799
5. Huang YY, Hou TY, Yu WK, et al. The clinical feature and treatment outcome of ocular melanoma: a 34-year experience in a tertiary referral center. Cancers (Basel). 2021;13(23):5926. doi: 10.3390/cancers13235926
6. Manchegowda P, Singh AD, Shields C, et al. Uveal Melanoma in Asians: A Review. Ocul Oncol Pathol. 2021;7(3):159-167. doi: 10.1159/000512738
7. Jager MJ, Shields CL, Cebulla CM, et al. Uveal melanoma. Nat Rev Dis Primers. 2020;6(1):24. doi: 10.1038/s41572-020-0158-0
8. Figueira E, Rajak S, McKelvie P, et al. Primary orbital melanoma: a case series and literature review. Orbit. 2018;37(5):352-357. doi: 10.1080/01676830.2017.1423354
9. El-Sawy T, Bakhoum MF, Tetzlaff M, et al. Primary orbital melanoma in association with cellular blue nevus. Digit J Ophthalmol. 2014;20(3):35-40. doi: 10.5693/djo.01.2014.02.001
10. Gentile C, Ranno MV, Salcedo Camargo SLL, et al. Extraocular extension in melanoma at an ocular oncology unit in Buenos Aires. Ocul Oncol Pathol. 2026;12(2):128–36. doi: 10.1159/000551168
11. Eagle RC, Grossniklaus HE, Syed N, et al. Inadvertent evisceration of eyes containing uveal melanoma. Arch Ophthalmol. 2009;127(2):141-5. doi: 10.1001/archophthalmol.2008.543
12. Tupynambá APFC, Heller HL, Britto MFL, et al. Progressive vision loss from uveal melanoma with extraocular extension: a case report. Am J Case Rep. 2025;26:e947979. doi: 10.12659/AJCR.947979
13. Ulas B, Ozcan AA, Celikten FA, et al. Prognostic insights into orbital metastases: a comprehensive analysis of clinical features and survival outcomes. Diagnostics (Basel). 2025;15(19):2542. doi: 10.3390/diagnostics15192542
14. Chetroiu D, Brouwer NJ, van den Berk M, et al. Prognosis and determinants of survival after orbital exenteration for conjunctival melanoma: experiences from a Dutch referral centre. Acta Ophthalmol. 2026;104(1):e95–103. doi: 10.1111/aos.17553
15. Riley DS, Barber MS, Kienle GS, et al. CARE guidelines for case reports: explanation and elaboration document. J Clin Epidemiol. 2017;89:218-235. doi: 10.1016/j.jclinepi.2017.04.026
16. Miyamoto C, Balazsi M, Bakalian S, et al. Uveal melanoma: Ocular and systemic disease. Saudi J Ophthalmol. 2012;26(2):145-9. doi: 10.1016/j.sjopt.2012.02.010
17. American Brachytherapy Society - Ophthalmic Oncology Task Force. The American Brachytherapy Society consensus guidelines for plaque brachytherapy of uveal melanoma and retinoblastoma. Brachytherapy. 2014;13(1):1-14. doi: 10.1016/j.brachy.2013.11.008
18. Niinimäki P, Määttänen M, Vuola J, et al. Orbital exenteration in the management of orbital and periorbital tumours: factors related to treatment outcomes. J Plast Reconstr Aesthet Surg. 2025;105:260–9. doi: 10.1016/j.bjps.2025.03.060
19. Baum SH, Westekemper H, Bechrakis NE, et al. Conjunctival and uveal melanoma: survival and risk factors following orbital exenteration. Eur J Ophthalmol. 2022;32(1):612–9. doi: 10.1177/1120672121995131
20. Liu X, Yue H, Jiang S, et al. Clinical features and prognosis of patients with metastatic ocular and orbital melanoma: a bi-institutional study. Cancer Med. 2023;12(15):16163–72. doi: 10.1002/cam4.6273
21. Zong C, Jia S, Zhu T, et al. Risk factors and prognosis of orbital exenteration in conjunctival melanoma. Eye (Lond). 2023;37(11):2272–80. doi: 10.1038/s41433-022-02330-w
22. Qedair J, Haider AS, Balasubramanian K, et al. Orbital exenteration for craniofacial lesions: a systematic review and meta-analysis of patient characteristics and survival outcomes. Cancers (Basel). 2023;15(17):4285. doi: 10.3390/cancers15174285
23. Harbour JW, Correa ZM, Schefler AC, et al. 15-gene expression profile and PRAME as integrated prognostic test for uveal melanoma: first report of Collaborative Ocular Oncology Group Study No. 2 (COOG2.1). J Clin Oncol. 2024;42(28):3319–29. doi: 10.1200/JCO.24.00447
24. Noguchi T, Ariga S, Moku R, et al. Actionable gene alterations identified in patients with malignant melanoma by targeted sequencing in Japan. JCO Precis Oncol. 2025;9:e2400437. doi: 10.1200/PO-24-00437
25. Miller M, Schoenfield L, Abdel-Rahman M, et al. Is Uveal Melanoma a Hormonally Sensitive Cancer? A Review of the Impact of Sex Hormones and Pregnancy on Uveal Melanoma. Ocul Oncol Pathol. 2021;7(4):239-250. doi: 10.1159/000514650
26. Schoenfield L, Janse S, Kline D, et al. Estrogen Receptor Is Expressed in Uveal Melanoma: A Potential Target for Therapy. Ocul Oncol Pathol. 2021;7(4):303-310. doi: 10.1159/000512174
27. Orozco CA, Mejía-García A, Ramírez M, et al. Validation of an ultraviolet light response gene signature for predicting prognosis in patients with uveal melanoma. Biomolecules. 2023;13(7):1148. doi: 10.3390/biom13071148
28. Caraviello C, Nazzaro G, Tavoletti G, et al. Melanoma skin cancer: a comprehensive review of current knowledge. Cancers (Basel). 2025;17(17):2920. doi: 10.3390/cancers17172920
29. Nayman T, Bostan C, Logan P, et al. Uveal Melanoma Risk Factors: A Systematic Review of Meta-Analyses. Curr Eye Res. 2017;42(8):1085-1093. doi: 10.1080/02713683.2017.1297997
30. Garg G, Finger PT, Kivelä TT, et al. Patients presenting with metastases: stage IV uveal melanoma, an international study. Br J Ophthalmol. 2022;106(4):510-517. doi: 10.1136/bjophthalmol-2020-317949
31. Wainstein AJ, Drummond-Lage AP, Kansaon MJ, et al. Sentinel lymph node biopsy for conjunctival malignant melanoma: surgical techniques. Clin Ophthalmol. 2015;9:1-6. doi: 10.2147/OPTH.S71226
32. Echegoyen JC, Hirabayashi KE, Lin KY, et al. Imaging of eyelid lymphatic drainage. Saudi J Ophthalmol. 2012;26(4):441-3. doi: 10.1016/j.sjopt.2012.08.003
33. Rantala ES, Hernberg MM, Piperno-Neumann S, et al. Metastatic uveal melanoma: The final frontier. Prog Retin Eye Res. 2022;90:101041. doi: 10.1016/j.preteyeres.2022.101041
34. Hanratty K, Finegan G, Rochfort KD, et al. Current treatment of uveal melanoma. Cancers (Basel). 2025;17(9):1403. doi: 10.3390/cancers17091403
35. Seth R, Agarwala SS, Messersmith H, et al. Systemic therapy for melanoma: ASCO guideline update. J Clin Oncol. 2023;41(30):4794–820. doi: 10.1200/JCO.23.01136
36. Nathan P, Hassel JC, Rutkowski P, et al. Overall survival benefit with tebentafusp in metastatic uveal melanoma. N Engl J Med. 2021;385(13):1196–206. doi: 10.1056/NEJMoa2103485
37. Hassel JC, Piperno-Neumann S, Rutkowski P, et al. Three-year overall survival with tebentafusp in metastatic uveal melanoma. N Engl J Med. 2023;389(24):2256–66. doi: 10.1056/NEJMoa2304753
38. Kim KB, Desprez PY, de Semir D, et al. Phase II study of niraparib in patients with advanced melanoma with homologous recombination pathway gene mutations. JCO Precis Oncol. 2025;9:e2400658. doi: 10.1200/PO-24-00658
39. Rogala P, Czarnecka AM, Dudzisz-Śledź M, et al. Current treatment standards for metastatic uveal melanoma. Cancers (Basel). 2026;18(3):475. doi: 10.3390/cancers18030475

40. Atun R, Jaffray DA, Barton MB, et al. Expanding global access to radiotherapy. Lancet Oncol. 2015;16(10):1153-86. doi: 10.1016/S1470-2045(15)00222-3
41. Jaarsma-Coes MG, Klaassen L, Marinkovic M, et al. Magnetic resonance imaging in the clinical care for uveal melanoma patients—a systematic review from an ophthalmic perspective. Cancers (Basel). 2023;15(11):2995. doi: 10.3390/cancers15112995
42. Solnik M, Paduszyńska N, Czarnecka AM, et al. Imaging of uveal melanoma—current standard and methods in development. Cancers (Basel). 2022;14(13):3147. doi: 10.3390/cancers14133147
43. Mouriaux F, Sanschagrin F, Diorio C, et al. Increased HIF-1α expression correlates with cell proliferation and vascular markers CD31 and VEGF-A in uveal melanoma. Invest Ophthalmol Vis Sci. 2014;55(3):1277-83. doi: 10.1167/iovs.13-13345
44. Brown IN, Lafita-Navarro MC, Conacci-Sorrell M. Regulation of Nucleolar Activity by MYC. Cells. 2022;11(3):574. doi: 10.3390/cells11030574
45. Matatall KA, Agapova OA, Onken MD, et al. BAP1 deficiency causes loss of melanocytic cell identity in uveal melanoma. BMC Cancer. 2013;13:371. doi: 10.1186/1471-2407-13-371
46. Lüke J, Vukoja V, Brandenbusch T, et al. CD147 and matrix-metalloproteinase-2 expression in metastatic and non-metastatic uveal melanomas. BMC Ophthalmol. 2016;16:74. doi: 10.1186/s12886-016-0222-4
47. Shamsoon K, Hiraki D, Yoshida K, et al. The Role of Hedgehog Signaling in the Melanoma Tumor Bone Microenvironment. Int J Mol Sci. 2023;24(10):8862. doi: 10.3390/ijms24108862
48. Baghaie L, Haxho F, Leroy F, et al. Contemporaneous Perioperative Inflammatory and Angiogenic Cytokine Profiles of Surgical Breast, Colorectal, and Prostate Cancer Patients: Clinical Implications. Cells. 2023;12(23):2767. doi: 10.3390/cells12232767
49. Knaul FM, Farmer PE, Krakauer EL, et al. Alleviating the access abyss in palliative care and pain relief-an imperative of universal health coverage: the Lancet Commission report. Lancet. 2018;391(10128):1391-1454. doi: 10.1016/S0140-6736(17)32513-8